Supporting Information

Ultra-pH Sensitive Nanoprobe Library with Broad pH Tunability and Fluorescence Emissions

Xinpeng Ma,[†,‡] Yiguang Wang,[†,‡]Tian Zhao,[†] Yang Li,[†] Lee-Chun Su,[†] Zhaohui Wang,[†] Gang Huang, [†]Baran D. Sumer[ξ] and Jinming Gao[*,†,&]

[†] Department of Pharmacology, [ξ]Department of Otolaryngology , Simmons Comprehensive Cancer Center, University of Texas Southwestern Medical Center, Dallas, Texas 75390, USA; [&]Department of Chemistry, University of Texas at Dallas, Richardson, Texas 75083, USA

[‡]These authors contributed equally to this work

*To whom correspondence should be addressed:

E-mail: jinming.gao@utsouthwestern.edu

Materials

The *N*-hydroxyl succinimidyl (NHS) esters of different fluorophores and fluorescence quenchers were obtained as following: RhoG-NHS, TMR-NHS, ROX-NHS, BDY-NHS, BDY-TMR-NHS, BDY630-NHS, AMCA-x-NHS, MB-NHS, PPO-NHS, QSY35, QSY7 and QSY21 ester from Invitrogen Company; Cy5-NHS, Cy5.5-NHS, Cy7.5-NHS ester from Lumiprobe Corporation; BHQ-1-NHS ester from Biosearch Technologies. PEO macroinitiator, MeO-PEO_{114}-Br, was prepared from 2-bromo-2-methyl propanoyl bromide and MeO-PEO_{114}-OH according to the procedure in the literature.[1] Bromopropane, bromobutane, bromopentane, ethanolamine and methacrylate chloride were purchased from Sigma-Aldrich. Monomers 2-(diethylamino)ethyl methacrylate (DEA-MA) and 2-aminoethyl methacrylate (AMA-MA) were purchased from Polyscience Company. AMA-MA was recrystallized twice with isopropanol and ethyl acetate (3:7). Monomer 2-(dibutylamino) ethyl methacrylate (DBA-MA) was synthesized following a previously published procedure.[2] Syntheses of 2-(dipropylamino) ethyl methacrylate (DPA-MA)and 2-(dipentylamino) ethyl methacrylate (D5A-MA) were reported recently.[3] Other solvents and reagents were used as received from Sigma-Aldrich or Fisher Scientific Inc.

Syntheses of PEO-*b*-PR block copolymers

PEO-*b*-PR copolymers were synthesized by atom transfer radical polymerization (ATRP) following similar procedures previously reported.[2] The dye free copolymers were used in polymer characterizations. PEO-*b*-PDPA is used as an example to illustrate the procedure. First, DPA-MA (1.70 g, 8 mmol), PMDETA (21 μL, 0.1 mmol) and MeO-PEO_{114}-Br (0.5 g, 0.1 mmol) were charged into a polymerization tube. Then a mixture of 2-propanol (2 mL) and DMF (2 mL) was added to dissolve the monomer and initiator. After three cycles of freeze-pump-thaw to remove the oxygen, CuBr (14 mg, 0.1 mmol) was added into the polymerization tube under nitrogen atmosphere, and the tube was sealed *in vacuo*. The polymerization was carried out at 40 °C for 8 hours. After polymerization, the reaction mixture was diluted with 10 mL THF, and passed through a neutral Al_2O_3 column to remove the catalyst. The THF solvent was removed by rotovap. The residue was dialyzed in distilled water and lyophilized to obtain a white powder. After syntheses, the polymers were characterized by ^{1}H NMR, ^{13}C NMR, gel permeation chromatography (GPC), differential scanning calorimetry (DSC) and thermal gravimetric analysis (TGA). All the NMR spectra were obtained in $CDCl_3$ using tetramethylsilane (TMS) as the internal reference on a Varian 400 MHz ^{1}H NMR spectrometer. GPC measurements were performed on a Viscotech GPCmax instrument using PLgel 5μm MIXED-D columns (Polymer Labs) and THF as eluent (1 mL/min). DSC analysis of copolymers was carried out using a Shimadzu Differential Scanning Calorimeter (DSC-60, Columbia, USA) with samples under a nitrogen atmosphere to determine the glass transition temperature (T_g) and melting temperature (T_m). DSC measurements were performed at a heating rate of 10˚C/min in the temperature range of -100˚C to 100 ˚C and sequential cooling back to -100 ˚C at a cooling rate of 50 ˚C/min, and then the sample was heated at a rate of 10 ˚C/min again. The data were analyzed using the TA software. T_g was calculated as the midpoint temperature during glass transition. TGA

experiments were conducted using a Perkin-Elmer TGA-4000 instrument (Waltham, MA) under a nitrogen atmosphere (flow rate: 20 mL/min). TGA measurements were performed at a heating rate of 20 ˚C/min in the temperature range of 30 ˚C to 500 ˚C. The onset degradation temperature (T_d, ˚C) and temperature with 50% weight loss (T_{50}) were determined by the Paris Data Analysis software.

The ^{1}H and ^{13}C NMR, DSC and TGA characterizations of all the copolymers are as following:

PEO-*b*-PD5A

^{1}H NMR (TMS, $CDCl_3$, ppm): 3.97 (b, 160H, $COOCH_2$), 3.79-3.50 (m, 450H, OCH_2CH_2O), 3.38 (s, 3H, CH_3O), 2.67 (b, 160H, $COOCH_2CH_2N$), 2.45 (b, 320H, NCH_2CH_2), 1.88-1.73 (m, 166H, CCH_3C& $C(CH_3)_2$), 1.43 (m, 320H, NCH_2CH_2), 1.32 (m, 320H, $NCH_2CH_2CH_2$), 1.27 (m, 320H, CH_2CH_3), 1.04 (b, 160H, CCH_3), 0.91 (m, 480H, CH_2CH_3). **^{13}C NMR** ($CDCl_3$, ppm):177.55, 177.16, 176.40, 71.88, 70.51, 63.08, 59.00, 58.51, 54.77, 54.66, 51.64, 45.9, 44.66, 29.62, 27.06, 22.64, 18.61, 18.30, 16.71, 14.14. See Table S3 for DSC and TGA data.

PEO-*b*-P(DEA_{20}-*r*-$D5A_{60}$)

^{1}H NMR (TMS, $CDCl_3$, ppm):): 3.98 (b, 160H, $COOCH_2$), 3.79-3.50 (m, 450H, OCH_2CH_2O), 3.38 (s, 3H, CH_3O), 2.67 (b, 160H, $COOCH_2CH_2N$), 2.57 (b, 40H, $COOCH_2CH_2NEt_2$), 2.44(b, 240H, NCH_2CH_2), 1.89-1.79 (m, 166H, CCH_2C& $C(CH_3)_2$), 1.43 (m, 240H, NCH_2CH_2), 1.32 (m, 240H, NCH_2CH_2 CH_2), 1.26 (b, 240H, $CH_2CH_2CH_3$), 1.04 (b, 240H, NCH_2CH_3), 0.91 (m, 520H, CCH_3 & $CH_2CH_2CH_3$).). **^{13}C NMR** ($CDCl_3$, ppm): 177.60, 177.21, 176.40, 71.86, 70.51, 63.11, 54.78, 54.66, 52.06, 51.63, 50.43, 47.58, 45.05, 44.67, 29.61, 27.07, 22.64, 18.60, 18.29, 16.92, 16.58, 14.14, 12.15. T_g: 0.55 ˚C. T_m: 49.3 ˚C. T_d: 258.8 ˚C. T_{50}: 394.8 ˚C.

PEO-*b*-P(DEA_{40}-*r*-$D5A_{40}$)

^{1}H NMR (TMS, $CDCl_3$, ppm):): 3.98 (b, 160H, $COOCH_2$), 3.81-3.50 (m, 450H, OCH_2CH_2O), 3.40 (s, 3H, CH_3O), 2.69 (b, 160H, $COOCH_2CH_2N$), 2.57 (b, 160H, $COOCH_2CH_2NEt_2$), 2.44(b, 160H, NCH_2CH_2), 1.89-1.79 (m, 166H, CCH_2C& $C(CH_3)_2$), 1.43 (m, 160H, NCH_2CH_2), 1.32 (m, 160H, NCH_2CH_2 CH_2), 1.25 (b, 160H, $CH_2CH_2CH_3$), 1.05 (b, 240H, NCH_2CH_3), 0.91 (m, 400H, CCH_3 & $CH_2CH_2CH_3$).). **^{13}C NMR** ($CDCl_3$, ppm): 177.62, 177.25, 176.46, 71.84, 70.50, 63.09, 56.70, 54.66, 54.14, 51.62, 50.41, 47.57, 45.02, 44.65, 29.61, 27.05, 22.63, 20.58, 18.48, 16.86, 16.60, 14.13, 12.12, 11.85. T_g: 1.2 ˚C. T_m: 45.1 ˚C. T_d: 265.2 ˚C. T_{50}: 400.1 ˚C.

PEO-*b*-P(DEA_{60}-*r*-$D5A_{20}$)

^{1}H NMR (TMS, $CDCl_3$, ppm):): 3.93 (b, 160H, $COOCH_2$), 3.72-3.44 (m, 450H, OCH_2CH_2O), 3.32 (s, 3H, CH_3O), 2.64 (b, 160H, $COOCH_2CH_2N$), 2.51 (b, 240H, $COOCH_2CH_2NEt_2$), 2.39 (b, 80H, NCH_2CH_2), 1.82-1.73 (m, 166H, CCH_2C& $C(CH_3)_2$), 1.38 (m, 80H, NCH_2CH_2), 1.27 (m, 80H, NCH_2CH_2 CH_2), 1.20 (b, 80H, $CH_2CH_2CH_3$), 0.99 (b, 360H, NCH_2CH_3), 0.85 (m, 280H,

C$C\mathit{H}_3$ & $CH_2CH_2C\mathit{H}_3$).). **^{13}C NMR** ($CDCl_3$, ppm): 177.67, 177.31, 176.46, 71.87, 70.45, 63.17, 58.99, 54.63, 54.13, 51.57, 50.38, 47.53, 45.02, 44.64, 29.59, 26.95, 22.60, 18.53, 16.82, 16.61, 14.11, 12.01. T_g: 1.9 ˚C. T_m: 45.7 ˚C. T_d: 276.3 ˚C. T_{50}: 407.7 ˚C.

PEO-*b*-PDEA

^{1}H NMR (TMS, $CDCl_3$, ppm): 3.93 (b, 160H, COO$C\mathit{H}_2$), 3.73-3.42 (m, 450H, O$C\mathit{H}_2C\mathit{H}_2$O), 3.31 (s, 3H, $C\mathit{H}_3$O), 2.64 (b, 166H, $COOCH_2C\mathit{H}_2N$), 2.51 (b, 320H, $NC\mathit{H}_2CH_3$), 1.82-1.73 (m, 160H, C$C\mathit{H}_2$C& C($C\mathit{H}_3$)$_2$), 1.18 (s, 6H, C($C\mathit{H}_3$)$_2$), 0.99 (m, $NCH_2C\mathit{H}_3$), 0.82 (b, 160H, C$C\mathit{H}_3$).). **^{13}C NMR** ($CDCl_3$, ppm): 177.61, 177.22, 176.44, 71.79, 70.42, 63.13, 58.89, 54.58, 54.10, 50.36, 50.30, 47.50, 44.93, 44.55, 29.52, 18.39, 16.73, 12.04. T_g: 2.3 ˚C. T_m: 56.4 ˚C. T_d: 287.8 ˚C. T_{50}: 418.8 ˚C.

PEO-*b*-PDBA

^{1}H NMR (TMS, $CDCl_3$, ppm): 3.91 (b, 160H, COO$C\mathit{H}_2$), 3.73-3.42 (m, 450H, O$C\mathit{H}_2C\mathit{H}_2$O), 3.31 (s, 3H, $C\mathit{H}_3$O), 2.60 (b, 166H, $COOCH_2C\mathit{H}_2N$), 2.38 (b, 320H, $NC\mathit{H}_2CH_2$), 1.82-1.72 (m, 160H, C$C\mathit{H}_3$C& C($C\mathit{H}_3$)$_2$), 1.35 (m, 320H, $NCH_2C\mathit{H}_2$), 1.25 (m, 320H, $CH2C\mathit{H}_2CH_3$), 0.97-0.84 (m, 640H, $CH_2C\mathit{H}_3$& C$C\mathit{H}_3$). **^{13}C NMR** ($CDCl_3$, ppm): 177.58, 177.19, 176.48, 71.90, 70.50, 63.08, 58.97, 57.47, 54.38, 52.03, 51.65, 45.05, 44.63, 29.55, 29.47, 20.51, 18.27, 16.79, 16.61, 14.08, 14.01. See Table S3 for DSC and TGA data.

PEO-*b*-P(DPA$_{20}$-*r*-DBA$_{60}$)

^{1}H NMR (TMS, $CDCl_3$, ppm): 3.97 (b, 160H, COO$C\mathit{H}_2$), 3.83-3.45 (m, 450H, O$C\mathit{H}_2C\mathit{H}_2$O), 3.38 (s, 3H, $C\mathit{H}_3$O), 2.67 (b, 166H, $COOCH_2C\mathit{H}_2N$), 2.44 (b, 320H, $NC\mathit{H}_2CH_2$), 1.80-1.68 (m, 160H, C$C\mathit{H}_3$C& C($C\mathit{H}_3$)$_2$), 1.42 (m, 320H, $NCH_2C\mathit{H}_2$), 1.30 (m, 240H, $NCH_2CH_2C\mathit{H}_2CH_3$), 1.04-0.87 (m, 640H, $CH_2C\mathit{H}_3$& C$C\mathit{H}_3$).). **^{13}C NMR** ($CDCl_3$, ppm): 177.63, 177.23, 176.47, 71.87, 70.51, 63.19, 63.13, 63.01, 56.71, 54.40, 51.67, 45.06, 44.65, 29.57, 20.58, 20.53, 18.51, 17.00, 16.64, 14.09, 11.84. T_g: 5.8 ˚C. T_m: 51.1 ˚C. T_d: 242.3 ˚C. T_{50}: 383.7 ˚C.

PEO-*b*-P(DPA$_{40}$-*r*-DBA$_{40}$)

^{1}H NMR (TMS, $CDCl_3$, ppm): 3.98 (b, 160H, COO$C\mathit{H}_2$), 3.83-3.45 (m, 450H, O$C\mathit{H}_2C\mathit{H}_2$O), 3.38 (s, 3H, $C\mathit{H}_3$O), 2.67 (b, 160H, $COOCH_2C\mathit{H}_2N$), 2.43 (b, 320H, $NC\mathit{H}_2CH_2$), 1.91-1.80 (m, 166H, C$C\mathit{H}_3$C& C($C\mathit{H}_3$)$_2$), 1.44 (m, 320H, $NCH_2C\mathit{H}_2$), 1.32 (m, 160H, $NCH_2CH_2C\mathit{H}_2CH_3$), 1.04-0.87 (m, 640H, $CH_2C\mathit{H}_3$& C$C\mathit{H}_3$).). **^{13}C NMR** ($CDCl_3$, ppm): 177.64, 177.26, 176.44, 70.46, 63.21, 63.07, 56.69, 54.48, 54.39, 51.71, 45.05, 44.64, 29.50, 20.53, 18.48, 18.33, 16.80, 16.46, 14.08, 11.83. T_g: 4.2 ˚C. T_m: 49.6 ˚C. T_d: 260.5 ˚C. T_{50}: 390.8 ˚C.

PEO-*b*-P(DPA$_{60}$-*r*-DBA$_{20}$)

^{1}H NMR (TMS, $CDCl_3$, ppm): 3.97 (b, 160H, COO$C\mathit{H}_2$), 3.82-3.47 (m, 450H, O$C\mathit{H}_2C\mathit{H}_2$O), 3.38 (s, 3H, $C\mathit{H}_3$O), 2.67 (b, 160H, $COOCH_2C\mathit{H}_2N$), 2.41 (b, 320H, $NC\mathit{H}_2CH_2$), 1.90-1.80 (m, 166H, C$C\mathit{H}_3$C& C($C\mathit{H}_3$)$_2$), 1.44 (m, 320H, $NCH_2C\mathit{H}_2$), 1.30 (m, 80H, $CH2C\mathit{H}_2CH_3$), 1.04-0.87

(m, 640H, CH_2CH_3& CCH_3). **^{13}C NMR** ($CDCl_3$, ppm): 177.67, 177.29, 176.54, 71.84, 70.46, 63.20, 63.06, 56.69, 54.47, 54.39, 51.70, 45.04, 44.64, 29.63, 29.48, 20.51, 18.48, 16.81, 16.57, 14.08, 11.83. See Table S3 for DSC and TGA data.

PEO-*b*-PDPA

^{1}H NMR (TMS, $CDCl_3$, ppm): 3.97 (b, 160H, $COOCH_2$), 3.83-3.47 (m, 450H, OCH_2CH_2O), 3.38 (s, 3H, CH_3O), 2.67 (b, 160H, $COOCH_2CH_2N$), 2.41 (b, 320H, NCH_2CH_2), 1.90-1.80 (m, 166H, CCH_3C& $C(CH_3)_2$), 1.44 (m, 320H, $NCH_2CH_2CH_3$), 1.04-0.87 (m, 640H, CH_2CH_3& CCH_3). **^{13}C NMR** ($CDCl_3$, ppm): 177.65, 177.27, 176.52, 71.85, 70.49, 63.20, 63.05, 58.96, 56.69, 54.14, 51.70, 45.02, 44.62, 29.61, 20.73, 20.56, 18.42, 16.55, 11.81. See Table S3 for DSC and TGA data.

PEO-*b*-P(DBA$_{28}$-*r*-D5A$_{52}$)

^{1}H NMR (TMS, $CDCl_3$, ppm): 3.97 (b, 160H, $COOCH_2$), 3.83-3.45 (m, 450H, OCH_2CH_2O), 3.38 (s, 3H, CH_3O), 2.67 (b, 160H, $COOCH_2CH_2N$), 2.44 (b, 320H, NCH_2CH_2), 1.89-1.80 (m, 166H, CCH_3C & $C(CH_3)_2$), 1.42 (m, 320H, NCH_2CH_2), 1.32 (m, 528H, $NCH_2CH_2CH_2CH_3$ & $NCH_2CH_2CH_2$ CH_2CH_3), 1.04-0.91 (m, 640H, CCH_3 & CH_2CH_3). **^{13}C NMR** ($CDCl_3$, ppm): 177.59, 177.18, 176.46, 71.89. 70.52, 63.63, 63.10, 54.67, 54.40, 51.65, 45.09, 44.67, 30.58, 29.62, 28.50, 27.07, 25.44, 25.12, 24.68, 22.65, 22.17, 20.55, 19.72, 18.58, 18.31, 18.19, 16.63, 15.47, 14.14. See Table S3 for DSC and TGA data.

PEO-*b*-P(DBA$_{56}$-*r*-D5A$_{24}$)

^{1}H NMR (TMS, $CDCl_3$, ppm): 3.97 (b, 160H, $COOCH_2$), 3.83-3.45 (m, 450H, OCH_2CH_2O), 3.38 (s, 3H, CH_3O), 2.67 (b, 160H, $COOCH_2CH_2N$), 2.46 (b, 320H, NCH_2CH_2), 1.89-1.79 (m, 166H, CCH_3C & $C(CH_3)_2$), 1.42 (m, 320H, NCH_2CH_2), 1.34 (m, 416H, $NCH_2CH_2CH_2CH_3$ & $NCH_2CH_2CH_2$ CH_2CH_3), 1.04-0.87 (m, 640H, CCH_3 & CH_2CH_3). **^{13}C NMR** ($CDCl_3$, ppm): 177.58, 177.18, 176.44, 71.87, 70.50, 63.12, 54.66, 54.39, 51.67, 45.07, 44.64, 29.58, 28.32, 27.05, 25.73, 25.42, 25.10, 22.62, 21.67, 20.52, 19.40, 18.56, 17.70, 16.59, 16.06, 14.09. See Table S3 for DSC and TGA data.

PEO-*b*-P(DPA$_{30}$-*r*-DBA$_{50}$)

^{1}H NMR (TMS, $CDCl_3$, ppm): 3.97 (b, 160H, $COOCH_2$), 3.83-3.45 (m, 450H, OCH_2CH_2O), 3.38 (s, 3H, CH_3O), 2.67 (b, 166H, $COOCH_2CH_2N$), 2.43 (b, 320H, NCH_2CH_2), 1.89-1.68 (m, 160H, CCH_3C & $C(CH_3)_2$), 1.42 (m, 320H, NCH_2CH_2), 1.32 (m, 200H, $NCH_2CH_2CH_2CH_3$), 1.04-0.87 (m, 640H, CH_2CH_3& CCH_3). **^{13}C NMR** ($CDCl_3$, ppm):177.64, 177.24, 176.52, 71.89, 70.52, 63.13, 59.00, 56.72, 54.42, 51.74, 51.68, 45.07, 44.66, 29.66, 29.58, 22.64, 20.59, 20.54, 18.51, 16.93, 16.63, 14.11, 11.85. See Table S3 for DSC and TGA data.

PEO-*b*-P(DEA$_{21}$-*r*-DPA$_{79}$)

^{1}H NMR (TMS, $CDCl_3$, ppm): 3.98 (b, 200H, COOCH_2), 3.83-3.47 (m, 450H, OCH_2CH_2O), 3.38 (s, 3H, CH_3O), 2.68 (b, 200H, COOCH$_2$CH_2N), 2.57 (b, 84H, NCH_2CH$_3$), 2.41 (b, 316H, NCH_2CH$_2$), 1.90-1.80 (m, 206H, CCH_3C & C(CH_3)$_2$), 1.46 (m, 316H, NCH$_2$CH_2CH$_3$), 1.05-0.89 (m, 900H, CH$_2$CH_3& CCH_3). **^{13}C NMR** ($CDCl_3$, ppm): 177.67, 177.28, 176.54, 71.86, 70.49, 63.21, 63.06, 56.69, 54.64, 54.18, 51.71, 50.38, 47.57, 45.02, 44.63, 29.62, 20.56, 18.42, 16.81, 16.55, 12.10, 11.82. See Table S3 for DSC and TGA data.

PEO-*b*-P(DEA$_{39}$-*r*-DPA$_{61}$)

^{1}H NMR (TMS, $CDCl_3$, ppm): 3.99 (b, 200H, COOCH_2), 3.83-3.45 (m, 450H, OCH_2CH_2O), 3.38 (s, 3H, CH_3O), 2.69 (b, 200H, COOCH$_2$CH_2N), 2.57 (b, 156H, NCH_2CH$_3$), 2.41 (b, 244H, NCH_2CH$_2$), 1.89-1.80 (m, 206H, CCH_3C & C(CH_3)$_2$), 1.45 (m, 244H, NCH$_2$CH_2CH$_3$), 1.05-0.87 (m, 900H, CH$_2$CH_3& CCH_3). **^{13}C NMR** ($CDCl_3$, ppm):177.63, 177.26, 176.51, 71.83, 70.47, 63.19, 63.04, 58.94, 56.66, 54.59, 54.22, 51.68, 50.40, 47.54, 44.98, 44.60, 29.58, 20.53, 18.41, 16.79, 16.49, 12.08, 11.80. See Table S3 for DSC and TGA data.

PEO-*b*-P(DEA$_{58}$-*r*-DPA$_{42}$)

^{1}H NMR (TMS, $CDCl_3$, ppm): 3.99 (b, 200H, COOCH_2), 3.83-3.45 (m, 450H, OCH_2CH_2O), 3.38 (s, 3H, CH_3O), 2.69 (b, 200H, COOCH$_2$CH_2N), 2.57 (b, 232H, NCH_2CH$_3$), 2.41 (b, 168H, NCH_2CH$_2$), 1.89-1.80 (m, 206H, CCH_3C & C(CH_3)$_2$), 1.46 (m, 168H, NCH$_2$CH_2CH$_3$), 1.04 (m, 474H, CH$_2$CH_3& CCH_3), 0.89 (m, 426H, CH$_2$CH_3& CCH_3). **^{13}C NMR** ($CDCl_3$, ppm): 177.66, 177.29, 176.52, 71.85, 70.48, 63.20, 63.05, 56.68, 54.17, 51.70, 50.41, 50.36, 47.56, 45.01, 44.62, 29.61, 20.55, 18.40, 16.71, 16.57, 12.10, 11.82. See Table S3 for DSC and TGA data.

Synthesis of triblock copolymer (PEG-*b*-P(R$_1$-*b*-R$_2$)) for control studies

PEG-*b*-P(R$_1$-*b*-R$_2$) triblock copolymers were synthesized by ATRP method following similar procedures previously reported.[2] PEO-*b*-P(D5A-*b*-DEA) is used as an example to illustrate the procedure. First, D5A-MA (0.54 g, 2 mmol), PMDETA (12μL, 0.05 mmol) and MeO-PEO$_{114}$-Br (0.25 g, 0.05 mmol) were charged into a polymerization tube. Then a mixture of 2-propanol (1 mL) and DMF (1 mL) was added to dissolve the monomer and initiator. After three cycles of freeze-pump-thaw to remove the oxygen, CuBr (7 mg, 0.05 mmol) was added into the polymerization tube under nitrogen atmosphere, and the tube was sealed *in vacuo*. After polymerization carrying out at 40 °C for 8 hours, deoxygenized DEA-MA (0.368, 2 mmol) was injected to the reaction solution via air-tight syringe and the reaction mixture was stirred at 40 °C for additional 8 hours. After polymerization, the reaction mixture was diluted with 10 mL THF, and passed through a neutral Al_2O_3 column to remove the catalyst. The THF solvent was removed by rotovap. The residue was dialyzed in distilled water and lyophilized to obtain a white powder. The ^{1}H NMR, ^{13}C NMR and GPC characterizations of the two copolymers are as following:

PEG-*b*-P(D5A-*b*-DEA)

^{1}H NMR (TMS, $CDCl_3$, ppm): 3.91 (b, 160H, $COOCH_2$), 3.75-3.40 (m, 450H, OCH_2CH_2O), 3.31 (s, 3H, CH_3O), 2.61 (b, 160H, $COOCH_2CH_2N$), 2.50 (b, 160H, $COOCH_2CH_2NEt_2$), 2.38(b, 160H, NCH_2CH_2), 1.82-1.74 (m, 166H, CCH_2C & $C(CH_3)_2$), 1.35 (b, 80H, NCH_2CH_2), 1.25 (m, 160H, $NCH_2CH_2CH_2$), 0.97 (b, 120H, NCH_2CH_3), 0.85 (m, 280H, CCH_3 & $CH_2CH_2CH_3$).). **^{13}C NMR** ($CDCl_3$, ppm): 177.52, 177.19, 176.35, 74.74, 71.80, 70.44, 63.09, 58.89, 56.64, 54.33, 51.46, 44.95, 44.55, 29.51, 20.51, 20.45, 18.43, 16.50, 14.07, 11.76. *Mn*: 22.1 kDa. PDI: 1.34.

PEG-*b*-P(DBA-*b*-DPA)

^{1}H NMR (TMS, $CDCl_3$, ppm): 3.91 (b, 160H, $COOCH_2$), 3.75-3.40 (m, 450H, OCH_2CH_2O), 3.31 (s, 3H, CH_3O), 2.61 (b, 160H, $COOCH_2CH_2N$), 2.38 (b, 320H, NCH_2CH_2), 1.87-1.74 (m, 166H, CCH_3C & $C(CH_3)_2$), 1.36 (m, 320H, NCH_2CH_2), 1.25 (m, 160H, $NCH_2CH_2CH_2CH_3$), 0.98-0.85 (m, 640H, CH_2CH_3& CCH_3).). **^{13}C NMR** ($CDCl_3$, ppm): 177.52, 177.19, 176.35, 71.80, 70.44, 63.09, 58.89, 56.64, 54.33, 51.64, 44.95, 44.55, 30.31, 29.51, 20.51, 20.45, 18.43, 16.78, 16.50, 14.02, 11.76. *Mn*: 20.9 kDa. PDI: 1.42.

Syntheses of PEO-*b*-(PR-*r*-Dye/FQ) block copolymers

AMA-MA was used for the conjugation of dyes or fluorescence quenchers. Synthesis of PEO-*b*-(PR-*r*-AMA) copolymers followed the procedure described above. Three primary amino groups were introduced into each polymer chain by controlling the feeding ratio of AMA monomer to the initiator (ratio = 3). After synthesis, PEO-*b*-(PR-*r*-AMA) (10 mg) was dissolved in 2 mL DMF. Then the NHS-ester (1.5 equivalences for Dye-NHS or FQ-NHS) was added. After overnight reaction, the copolymers were purified by preparative gel permeation chromatography (PLgel Prep 10 m 10E3 Å 300×250 columns by Varian, THF as eluent at 5 mL/min) to remove the free dye molecules. The produced PEO-*b*-(PR-*r*-Dye/FQ) copolymers were lyophilized and kept at -20 °C for storage.

Preparation and Characterization of micelle nanoparticles

Micelles were prepared following a previously published procedure.[2] In a typical procedure, 5 mg of **PDPA-Cy5** was dissolved in 0.5 mL THF. Then, the solution was slowly added into 4 mL of Milli-Q deionized water under sonication. The mixture was filtered 4 times to remove THF using the micro-ultrafiltration system (MWCO = 100 KD). Then, the deionized water was added to adjust the polymer concentration to 5 mg/mL as a stock solution. For the mixed micelles, different weight ratios of the PR-Dye and PR-FQ copolymers were dissolved in 0.5 mL THF, and the same procedure was used. After micelle formation, the nanoparticles were characterized by transmission electron microscopy (TEM, JEOL 1200 EX model, Tokyo, Japan) to examine micelle size and morphology, dynamic light scattering (DLS, Malvern Nano-ZS model, He-Ne laser, λ= 633 nm) for hydrodynamic diameter (D_h). The zeta-potential was measured using a folded capillary cell (Malvern Instruments, Herrenberg, Germany). The presented data were averaged from three independent measurements.

Fluorescence characterization

The fluorescence emission spectra were obtained on a Hitachi fluorometer (F-7500 model, Tokyo, Japan). For each copolymer, the sample was initially prepared in Milli-Q water at the concentration of 2 mg/mL. Then the stock solution was diluted in 0.2 M citric-phosphate buffers (containing 0.15 M sodium chloride) at different pH values. The terminal polymer concentration was controlled at 100-200 μg/mL.

The fluorescent images of **4.4-7.1-Cy5s**, **5.0-BDY**, **5.3-RhoG**, **5.6-TMR**, **5.9-ROX**, **6.2-BDY630**, **6.5-Cy5**, **6.8-Cy5.5** and **7.1-Cy7.5** solutions at different pH values (100 μg/mL for each sample) were obtained using the Maestro imaging system (CRI, Inc., Woburn, MA) with a proper band pass excitation filter and long-pass emission filter according to the instrument manual. For **4.4-AMCA** and **4.7-MB** solutions, the images were taken by a camera under the irradiation of a handheld UV light (365 nm). All measurements were conducted at room temperature.

Measurement of dye conjugation efficiency

The dye conjugation number and efficiency were determined by a UV-Vis method. Typically, solutions of the dye reference standard and polymer test samples in methanol were prepared. Then, the absorbance of the standard and sample solutions was determined at corresponding peak wavelength. The dye conjugation number and efficiency were calculated using the following equations:

$$N_{dye} = \frac{C_{dye}}{A_{dye}} \frac{A_{polymer}}{C_{polymer}} \frac{MW_{polymer}}{MW_{dye}}$$

$$Efficiency\ (\%) = \frac{N_{dye}}{N_{NH2}} \times 100\%$$

Where N_{dye} and N_{NH2} are the conjugated dye number and number of primary amine in the polymer; A_{dye} and $A_{polymer}$ are the absorbance of dye reference standard and polymer test sample, respectively; C_{dye} and $C_{polymer}$ are the concentrations of dye reference standard and polymer test sample, respectively; MW_{dye} and $MW_{polymer}$ are the molecular weights of dye reference standard and polymer test sample, respectively.

Quantum yields of fluorescent nanoprobes

The relative fluorescent quantum yield is measured via the comparative method described in the literature[4]. To simplify the test, the well characterized standards of known Φ_F were used as reference for the determination of quantum yield of dye-conjugated polymers. The reference dyes chosen for conjugation include Marina blue, BDY493, TMR, and Cy5, which have reported quantum yields of 0.89, 0.90, 0.68, and 0.28 in methanol, respectively[5-7].

For the quantum yield measurement, the free dyes and dye-conjugated polymers were dissolved and diluted in methanol to keep the absorbance of the solution less than 0.05. Then, the fluorescence spectra of the prepared samples were measured using an excitation wavelength

same as the absorbance wavelength. The integrated fluorescence intensities of the two solutions were calculated from the spectra. The quantum yield of the dye-conjugated polymers was calculated using the following equation:

$$\Phi_F = \Phi_{F,R} \frac{I}{OD} \frac{OD_R}{I_R} \frac{n^2}{n_R^2}$$

Where Φ_F is the fluorescent quantum yield, I is the integrated emission intensities, OD is the absorbance, n is the refractive index of the solvent, and the subscript R denotes the values for the reference sample.

Nanoprobe stability in serum and solutions containing serum components

Fresh mouse serum was collected and filtered through 0.22 μm syringe filters. Mouse serum components, including albumin and γ-globulin were obtained from Sigma-Aldrich Inc. Typically, 40 μL of nanoprobe (5 mg/mL) was added to 1 ml of serum or serum components. The mixture was incubated at 37ºC in a humidified chamber. At each designated time point, 100 μL aliquots of mixture were collected and immediately determined at pH 7.4 and pH 5.0 on a Hitachi fluorometer (F-7500 model, Tokyo, Japan) to calculate the fluorescence activation ratios.

Cytotoxicity analysis of polymer nanoprobes

H2009 lung cancer cells were plated onto 96-well plates at a density of 10,000 cells/well and incubated in the RPMI 1640 medium containing 5% fetal bovine serum (FBS) at 37 ºC, 5% CO_2/95% air to allow cell growth for 24 hours. Then the cells were exposed to increasing concentrations of a series of polymer nanoprobes for 4 hours and washed three times with PBS, and the fresh medium was added into plates. The cells were incubated for 48 hours before determination of cell viability. The cell viability was measured using an MTT assay. Briefly, after drug exposure, the cells were incubated with 0.5 mg/mL MTT solution for 4 hours, after which the medium was removed. Two hundred μL of DMSO was added into cell plates for OD determination at 570 nm using a microplate reader (SpectraMax M5, Molecular Devices, CA) to determine the dose-response relationships.

Confocal imaging of nanoprobe uptake in H2009 cells

H2009 lung cancer cells were plated in glass bottom dishes (MatTek, MA) in 1 mL phenol red-free RPMI medium and incubated with nanoprobes, including probe 6.2-BDY493 W/WO BHQ1 as well as probe 6.2-MB W/WO QSY35, at a polymer concentration of 200 μg/mL at pH 7.4. Confocal images were captured 60 min after addition of nanoprobes using the Nikon ECLIPSE TE2000-E confocal microscope with a 100× objective lens. MB and BDY493 were excited at 405 and 488 nm, respectively. The emission wavelengths of MB and BDY493 were 460 and 515 nm, respectively. The images were analyzed using Image-J software. Five independent measurements were presented as the mean ± standard deviation.

Reference

1. Bronstein, L. M.; Sidorov, S. N.; Zhirov, V.; Zhirov, D.; Kabachii, Y. A.; Kochev, S. Y.; Valetsky, P. M.; Stein, B.; Kiseleva, O. I.; Polyakov, S. N.; Shtykova, E. V.; Nikulina, E. V.; Svergun, D. I.; Khokhlov, A. R., *J. Phys. Chem. B* **2005,***109* (40), 18786-98.
2. Zhou, K.; Wang, Y.; Huang, X.; Luby-Phelps, K.; Sumer, B. D.; Gao, J., Tunable, Ultra-Sensitive pH Responsive Nanoparticles Targeting Specific Endocytic Organelles in Living Cells.*Angew. Chem. Int. Ed. Engl.* **2011,***50* (27), 6109-14.
3. Yang L, Wang YG, Huang G, Ma X, Gao J. A Surprising Chaotropic Anion-Induced Supramolecular Self-Assembly of Ionic Polymeric Micelles. *Angew. Chem. Int. Ed.* DOI: 10.1002/anie.201402525.
4. Lakowicz J.R., Principles of Fluorescence Spectroscopy, 2nd Ed., Kluwer Academic, New York, 1999.
5. Toomre, D. & Manstein, D.J. Lighting up the cell surface with evanescent wave microscopy. *Trends in cell biology* 2001, 11, 298-303.
6. Haugland, R.P. A guide to fluorescent probes and labeling technologies. 10th Edition. Invitrogen, San Diego, 2005.
7. Sun, W.C., Gee, K.R. & Haugland, R.P. Synthesis of novel fluorinated coumarins: excellent UV-light excitable fluorescent dyes. Bioorganic & medicinal chemistry letters 1998, 8, 3107-3110.

Table S1. Coarse-tuned pH sensitive nanoprobes from Cy5-conjugated **PEO-P(DEA$_x$-D5A$_y$)** copolymers.

Polymers	M_n (kDa)	M_w (kDa)	PDI	Yield (%)	pK$_a$	pH$_t$	ΔpH$_{10\text{-}90\%}$
PD5A	26.9	32.6	1.21	85	4.25	4.38	0.19
P(DEA$_{20}$-D5A$_{60}$)	21.3	26.3	1.23	90	5.20	5.19	0.65
P(DEA$_{40}$-D5A$_{40}$)	21.3	25.8	1.20	95	6.07	5.99	0.64
P(DEA$_{60}$-D5A$_{20}$)	22.3	26.4	1.19	90	6.70	6.88	0.47
PDEA	22.6	26.6	1.18	91	7.43	7.83	0.14

Table S2. Fine-tuned pH sensitive nanoprobes from Cy5-conjugated **PEO-P(DPA$_x$-DBA$_y$)** copolymers.

Polymers	M_n (kDa)	M_w (kDa)	PDI	Yield (%)	pK$_a$	pH$_t$	ΔpH$_{10\text{-}90\%}$
PDBA	22.5	26.8	1.19	80	5.17	5.27	0.20
P(DPA$_{20}$-DBA$_{60}$)	19.7	21.4	1.09	94	5.40	5.46	0.19
P(DPA$_{40}$-DBA$_{40}$)	21.7	24.7	1.14	78	5.63	5.70	0.20
P(DPA$_{60}$-DBA$_{20}$)	23.9	27.9	1.17	83	5.81	5.91	0.18
PDPA	22.6	27.3	1.21	91	6.18	6.21	0.20

Table S3. Characterization of the copolymers from the UPS library spanning the pH range from 4.4 to 7.4.

Probe	Composition	M_n (kDa)	M_w (kDa)	PDI	Yield (%)	T$_g$ (°C)	T$_m$ (°C)	T$_d$ (°C)	T$_{50}$ (°C)
4.4	PD5A	26.9	32.6	1.21	85	3.2	42.0	247.1	379.6
4.7	P(DBA$_{28}$-D5A$_{52}$)	20.2	23.3	1.15	82	3.0	42.3	249.8	395.4
5.0	P(DBA$_{56}$-D5A$_{24}$)	20.0	25.9	1.29	84	-[a]	44.4	257.7	396.8
5.3	PDBA	22.5	26.8	1.19	80	2.5	44.9	259.1	425.5
5.6	P(DPA$_{30}$-DBA$_{50}$)	20.4	24.9	1.22	89	3.7	48.1	253.3	400.6
5.9	P(DPA$_{60}$-DBA$_{20}$)	23.9	27.9	1.17	83	-1.9	47.9	258.8	386.2
6.2	PDPA	20.1	23.3	1.21	91	4.0	58.7	244.6	403.3
6.5	P(DEA$_{21}$-DPA$_{79}$)	21.8	24.3	1.12	87	0.16	45.4	267.2	402.3
6.8	P(DEA$_{39}$-DPA$_{61}$)	20.3	23.2	1.14	82	1.2	47.4	278.2	411.2
7.1	P(DEA$_{58}$-DPA$_{42}$)	23.1	25.2	1.09	85	0.20	47.1	280.3	406.7
7.4	P(DEA$_{76}$-DPA$_{24}$)	22.5	25.4	1.13	87	1.2	48.1	283.0	414.4

[a] Not detectable

Table S4. Characterization of the Cy5-conjugated nanoprobes from the UPS library.

Probe	Composition	D_h (nm)	PDI	Zeta-potential (mV)	pK_a	pH_t	$\Delta pH_{10\text{-}90\%}$
4.4	PD5A	50.8 ± 3.0	0.13	-0.6 ± 1.2	4.25	4.38	0.19
4.7	$P(DBA_{28}\text{-}D5A_{52})$	68.9 ± 2.6	0.09	-0.3 ± 0.6	4.58	4.67	0.15
5.0	$P(DBA_{56}\text{-}D5A_{24})$	63.2 ± 3.2	0.09	-2.0 ± 1.0	4.93	4.96	0.18
5.3	PDBA	43.5 ± 6.6	0.13	-1.3 ± 1.1	5.17	5.27	0.20
5.6	$P(DPA_{30}\text{-}DBA_{50})$	55.7 ± 1.4	0.12	-1.1 ± 0.7	5.60	5.63	0.19
5.9	$P(DPA_{60}\text{-}DBA_{20})$	49.3 ± 2.7	0.11	-0.2 ± 0.6	5.81	5.91	0.18
6.2	PDPA	46.8 ± 2.0	0.12	-0.3 ± 0.7	6.18	6.21	0.20
6.5	$P(DEA_{21}\text{-}DPA_{79})$	45.6 ± 3.3	0.12	0.4 ± 1.4	6.46	6.45	0.19
6.8	$P(DEA_{39}\text{-}DPA_{61})$	36.2 ± 1.6	0.13	-2.0 ± 0.7	6.76	6.76	0.20
7.1	$P(DEA_{58}\text{-}DPA_{42})$	35.6 ± 2.4	0.17	-1.1 ± 1.3	7.03	7.08	0.21
7.4	$P(DEA_{76}\text{-}DPA_{24})$	33.5 ± 1.8	0.14	-0.8 ± 0.5	7.31	7.44	0.18

Table S5. Characterization of two representative nanoprobes in PBS and medium at pH 7.4 and 5.0.

Nanoprobe	Solution	pH	D_h (nm)	PDI	Zeta-potential (mV)
$P(DEA_{40}\text{-}D5A_{40})$	PBS	7.4	29.4 ± 3.4	0.12	-1.5 ± 2.2
		5.0	9.2 ± 0.4	-	4.4 ± 2.4
	Medium	7.4	33.2 ± 4.4	0.10	-1.1 ± 0.7
		5.0	n.d.[a]	n.d.[a]	14.6 ± 2.6
$P(DPA_{40}\text{-}DBA_{40})$	PBS	7.4	36.3 ± 2.4	0.24	0.4 ± 0.7
		5.0	7.3 ± 0.7	-	9.8 ± 2.8
	Medium	7.4	36.8 ± 3.1	0.21	-1.1 ± 0.3
		5.0	n.d.[a]	n.d.[a]	13.4 ± 1.1

[a] Not detected due to the interference from serum proteins.

Table S6. Measurement of conjugation efficiency and quantum yields of dye-conjugated **PDPA** polymers.

Dyes	Dye conjugation		Quantum yield (Φ_F)[a]		
	Number	Efficiency (%)	Free dye[b]	Conjugated dye	Mixture[d]
Marina Blue	2.1	71	0.89	0.73	0.87
BODIPY 493/503	2.0	68	0.90	0.10/0.87[c]	0.86
TMR	2.2	72	0.68	0.15	0.64
Cy5	2.0	68	0.28	0.28	0.28

[a] In methanol unless noted otherwise. [b] Obtained from literature. [c] In methanol with 0.5% 1 M HCl. [d] Mixture of free dye with dye-free PDPA copolymer.

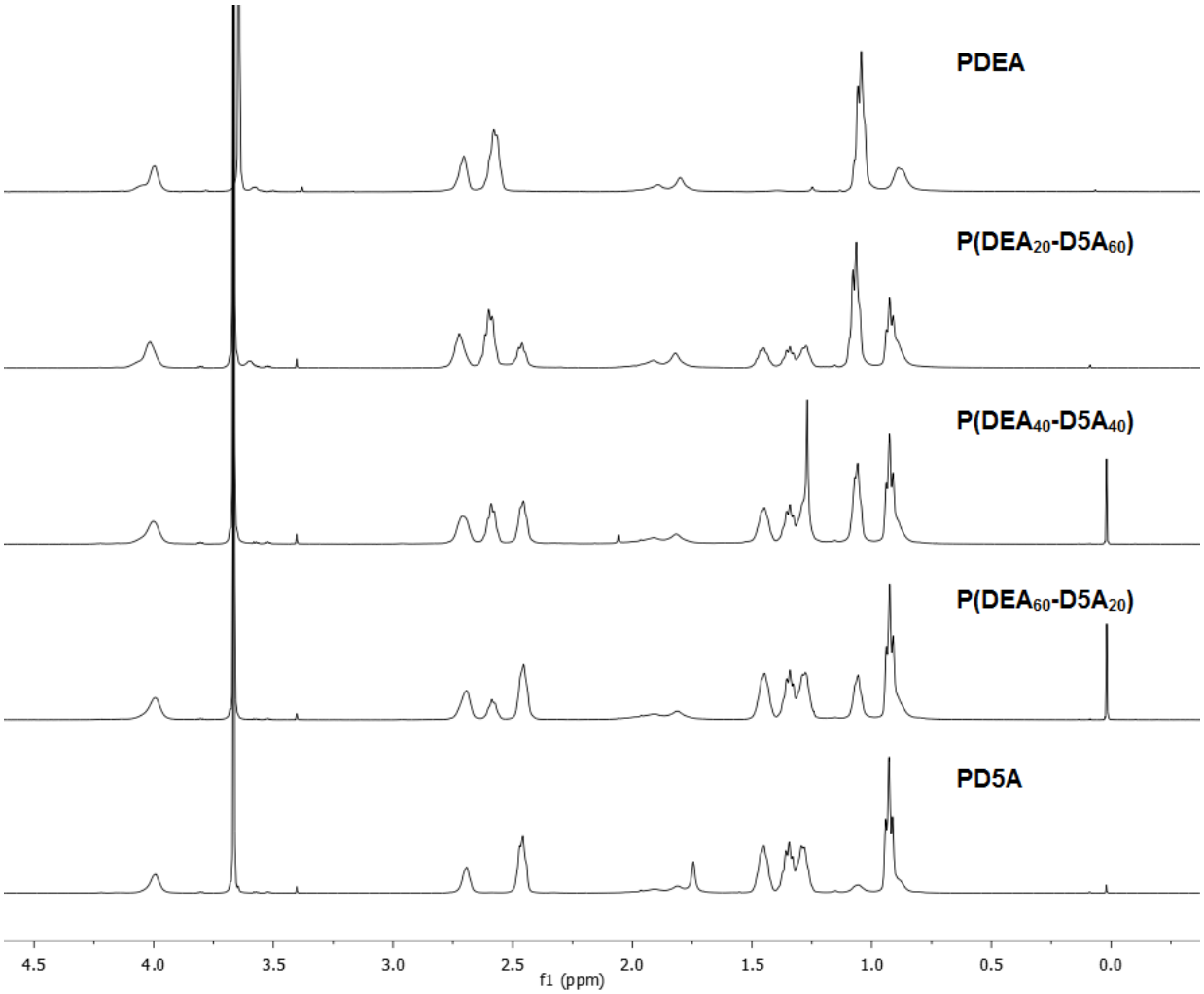

Figure S1. ^{1}HNMR spectra of **PEO-P(DEA$_x$-D5A$_y$)** (x + y = 80) copolymers at different monomer (DEA-MA and D5A-MA) ratios in the random copolymers. The peaks at 0.9 ppm and 1.1 ppm were used to estimate the monomer composition in the hydrophobic PR block.

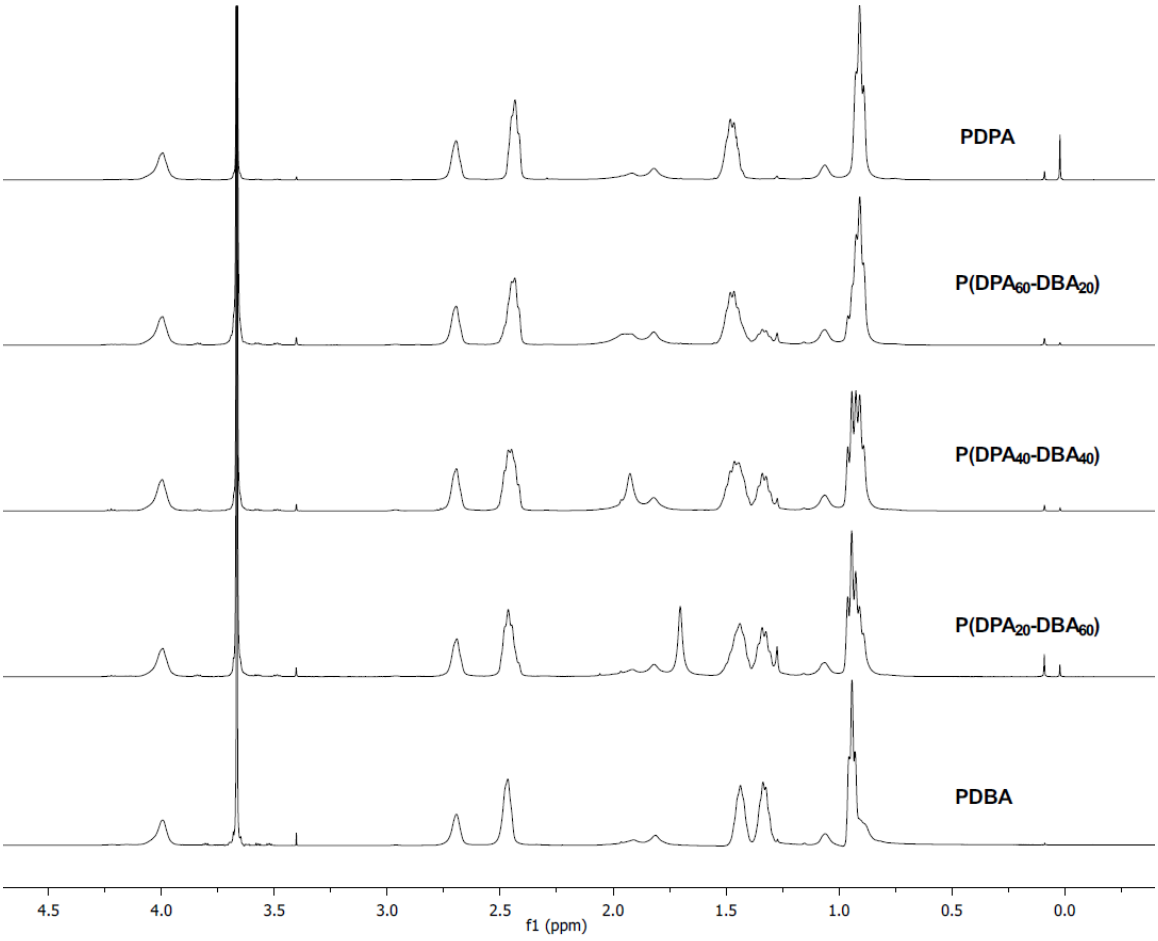

Figure S2. ^{1}HNMR spectra of **PEO-P(DPA$_x$-DBA$_y$)** (x + y = 80) copolymers at different monomer (DPA-MA and DBA-MA) ratios in the random copolymers. The peaks at 1.3 ppm and 1.4 ppm were used to estimate the monomer composition in the hydrophobic PR block.

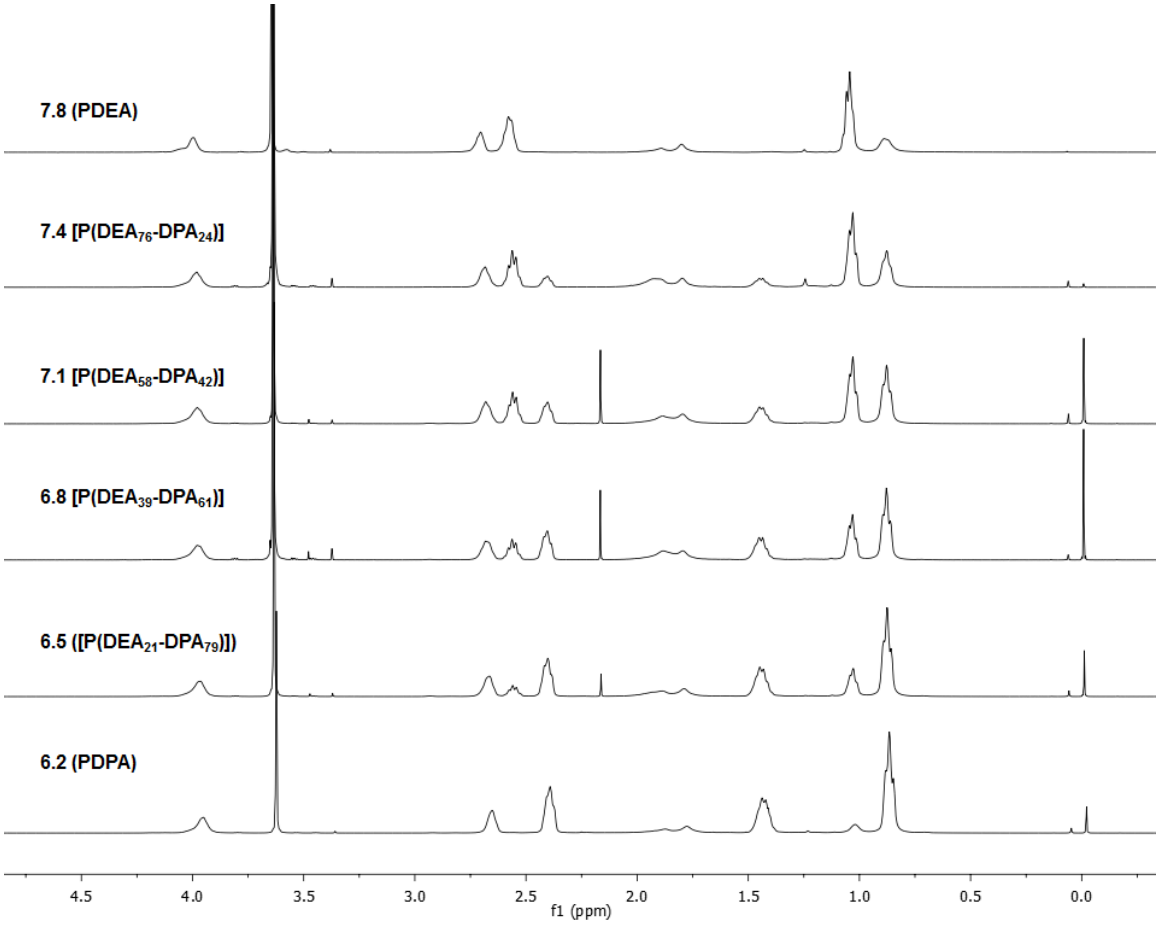

Figure S3. ^{1}HNMR spectra of nanoprobe compositions with pH_t values at 7.8, 7.4, 7.1, 6.8, 6.5 and 6.2 by adjusting the monomer (DEA-MA and DPA-MA) ratios in the hydrophobic PR block. The peaks at 0.9 ppm and 1.0-1.1 ppm were used to estimate the monomer composition in the hydrophobic PR block.

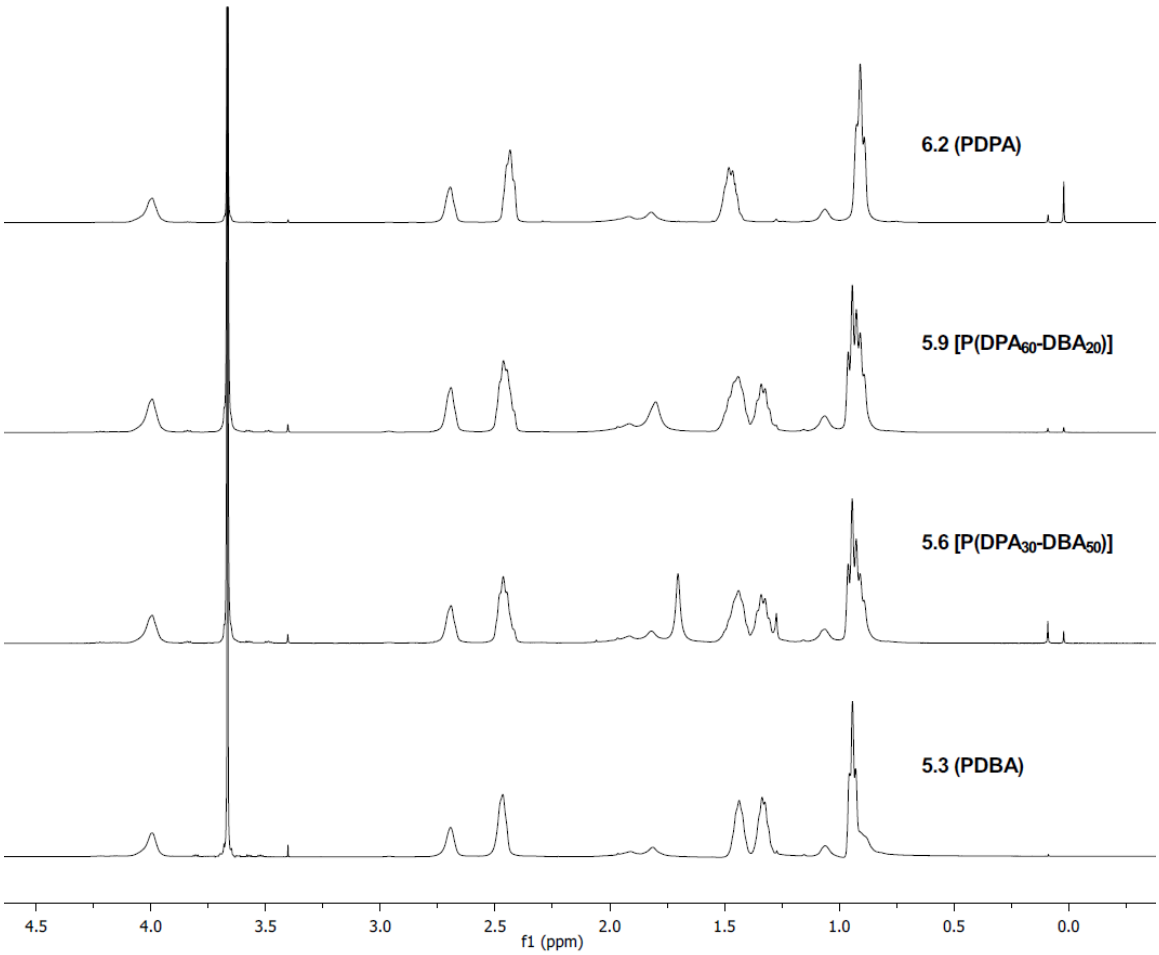

Figure S4. ^{1}HNMR spectra of nanoprobe compositions with pH_t values at 6.2, 5.9, 5.6 and 5.3 by adjusting the monomer (DPA-MA and DBA-MA) ratios in the hydrophobic PR block. The peaks at 1.3 ppm and 1.4 ppm were used to estimate the monomer composition in the hydrophobic PR block.

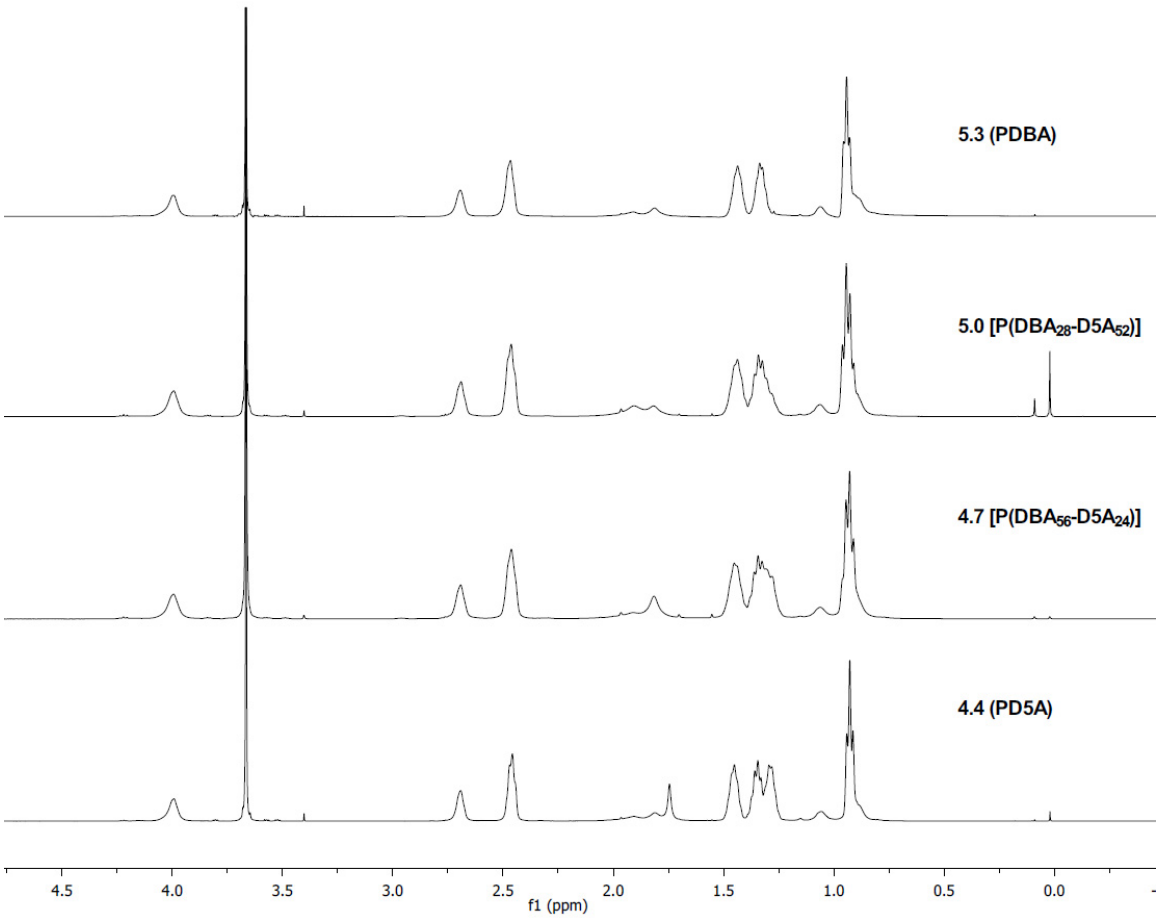

Figure S5. [1]HNMR spectra of nanoprobe compositions with pH_t values at 5.3, 5.0, 4.7 and 4.4 by adjusting the monomer (DBA-MA and D5A-MA) ratios in the hydrophobic PR block. The peaks at 1.3 ppm and 1.4 ppm were used to estimate the monomer composition in the hydrophobic PR block.

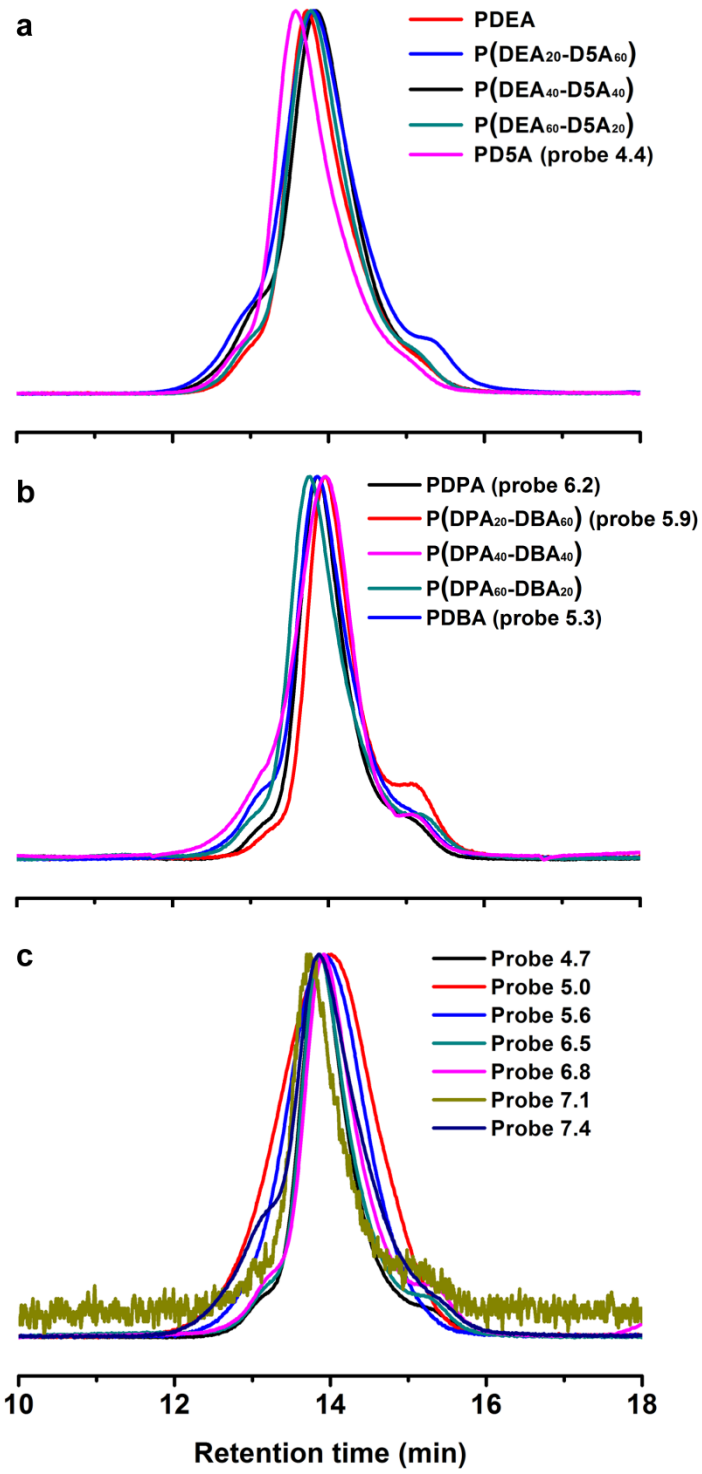

Figure S6. GPC chromatograms of all the copolymers. (**a**) P(DEA$_x$-D5A$_y$) series; (**b**) P(DPA$_x$-DBA$_y$) series; and (**c**) nanoprobes 4.7, 5.0, 5.6, 6.5, 6.8, 7.1 and 7.4.

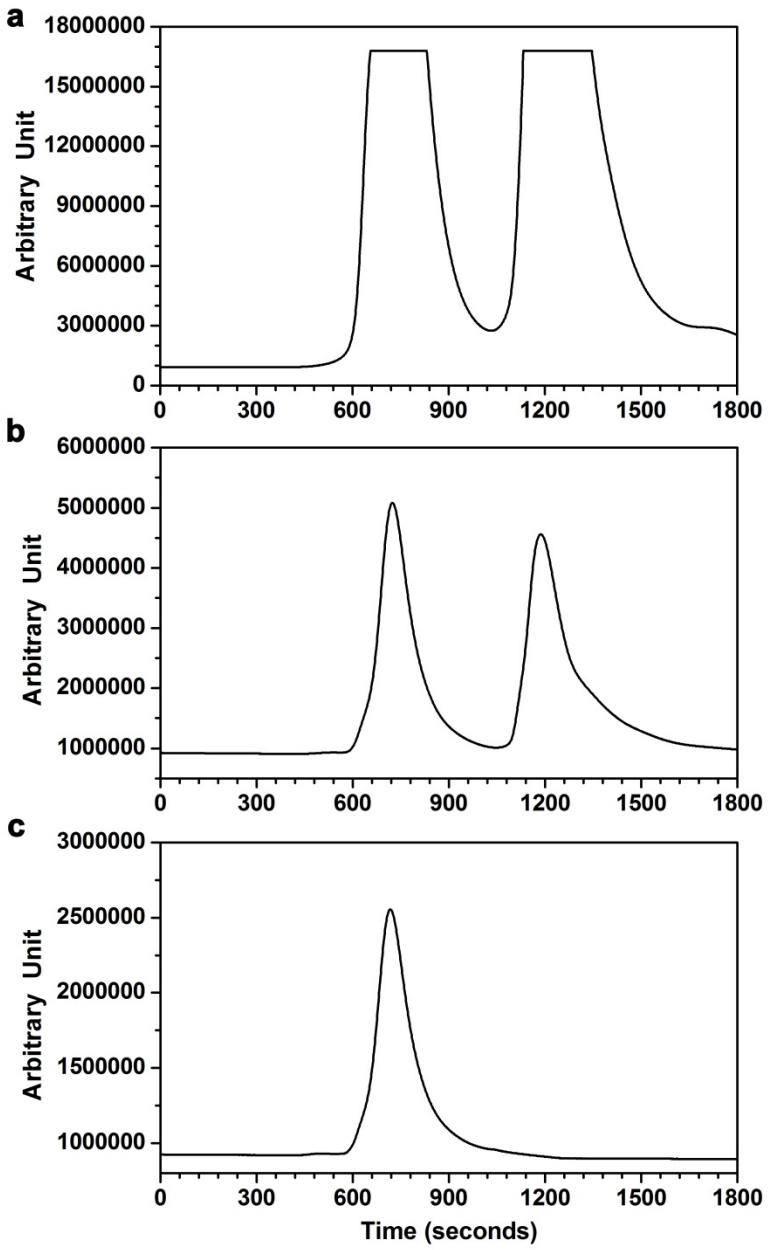

Figure S7. GPC chromatograms for the purification of dye-conjugated polymers. (**a**) Representative preparative GPC of **PDPA-TMR** synthetic mixture during purification (peak at elution time 700s is from PDPA-TMR and peak at 1200s is from the free TMR). Polymer fraction (600-900 s) was collected. (**b**) Analytical GPC of low concentration of **PDPA-TMR** synthetic mixture. (**c**) Analytical GPC of purified **PDPA-TMR** polymer showing the complete removal of free dye.

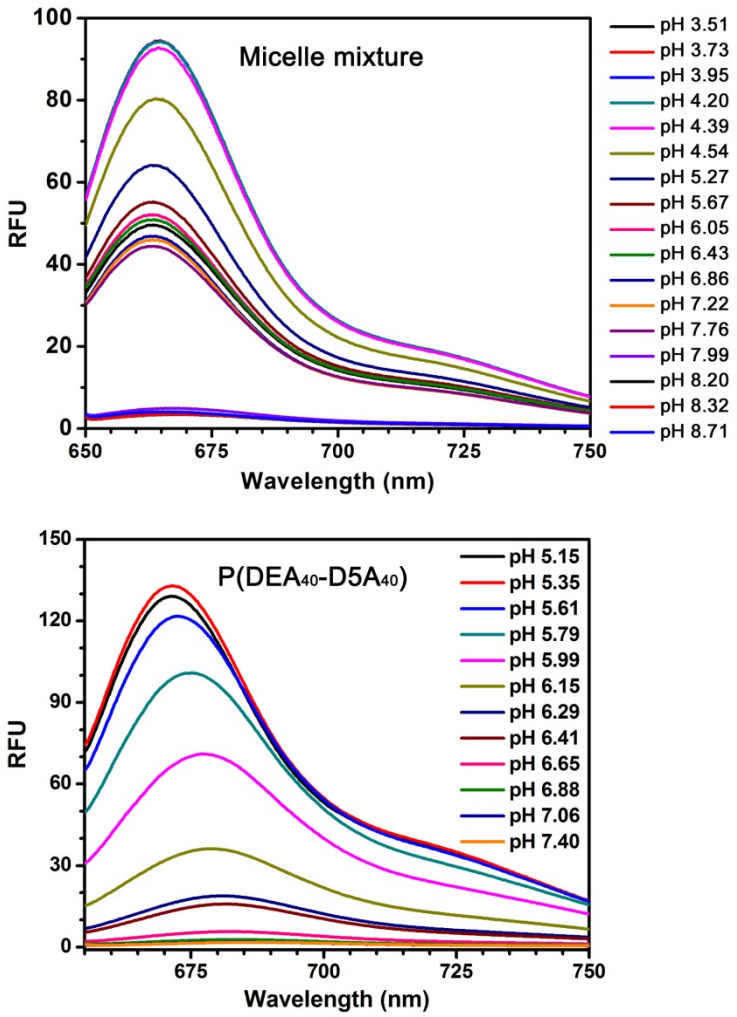

Figure S8. pH-dependent fluorescence spectra of **PDEA/PD5A** micelle mixture vs. **P(DEA$_{40}$-D5A$_{40}$)** copolymer nanoprobes. Cy5 dye ($\lambda_{ex}/\lambda_{em}$ = 646/662 nm) was conjugated to the PR blocks of the corresponding copolymers. The normalized fluorescence intensity vs. pH relationships were shown in **Figure 3a** in the main text.

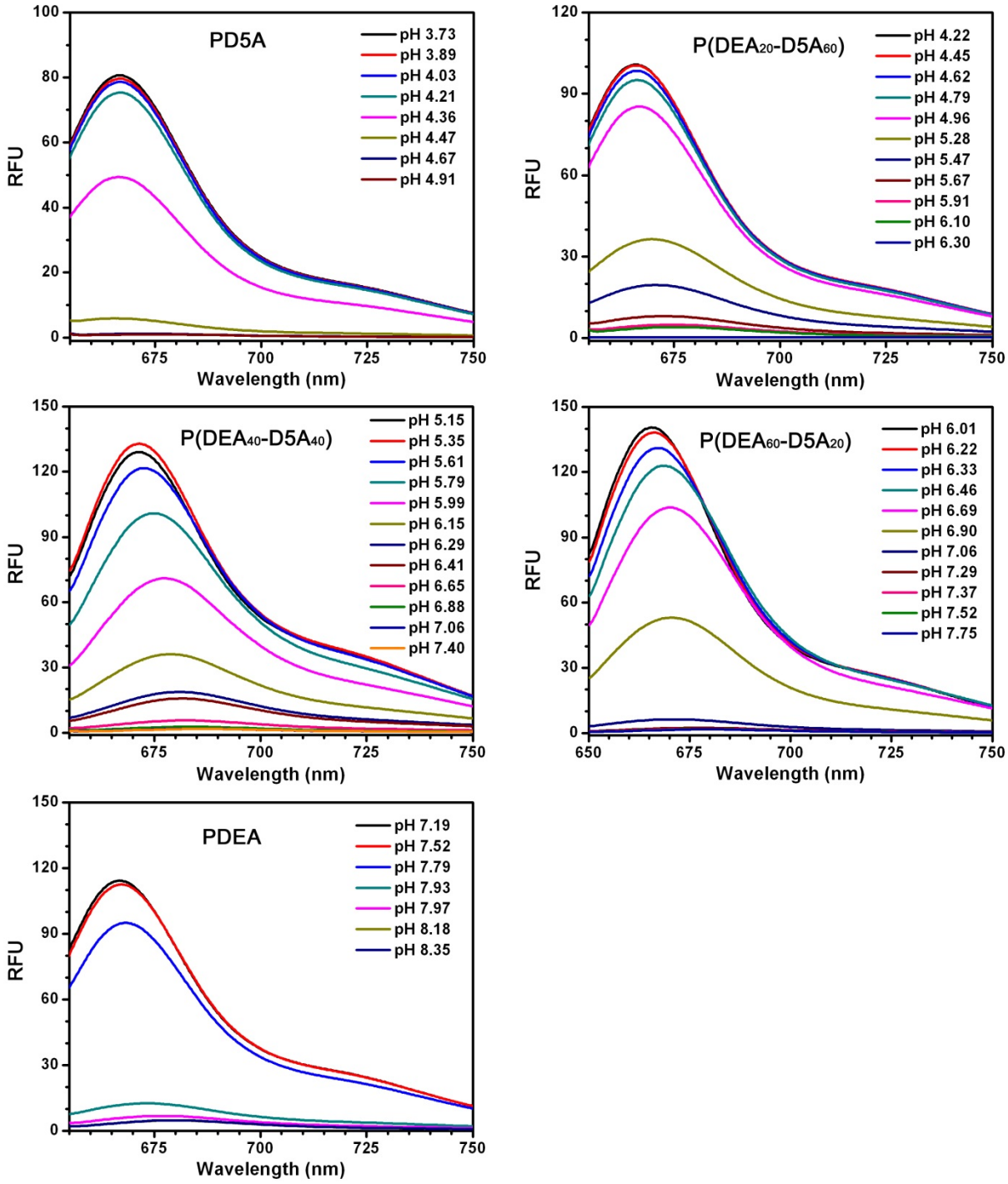

Figure S9. pH-dependent fluorescence spectra of coarse-tuned **P(DEA$_x$-D5A$_y$)** nanoprobes. Cy5 dye ($\lambda_{ex}/\lambda_{em}$ = 646/662 nm) was conjugated to the PR blocks of the copolymers. The normalized fluorescence intensity vs. pH relationships were shown in **Figure 3b** in the main text.

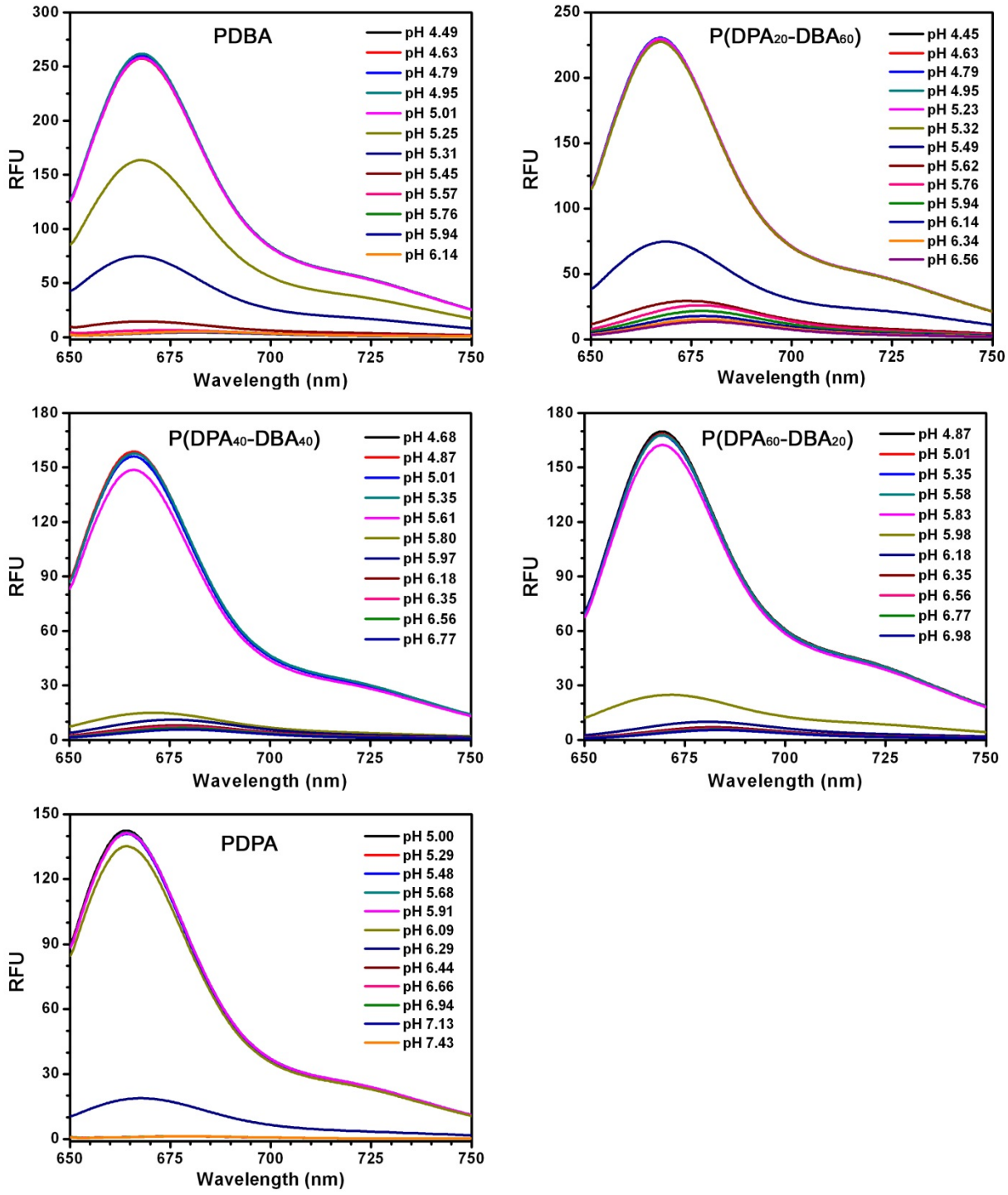

Figure S10. pH-dependent fluorescence spectra of fine-tuned **P(DPA$_x$-DBA$_y$)** nanoprobes. Cy5 dye ($\lambda_{ex}/\lambda_{em}$ = 646/662 nm) was conjugated to the PR blocks of the copolymers. The normalized fluorescence intensity vs. pH relationships were shown in **Figure 4a** in the main text.

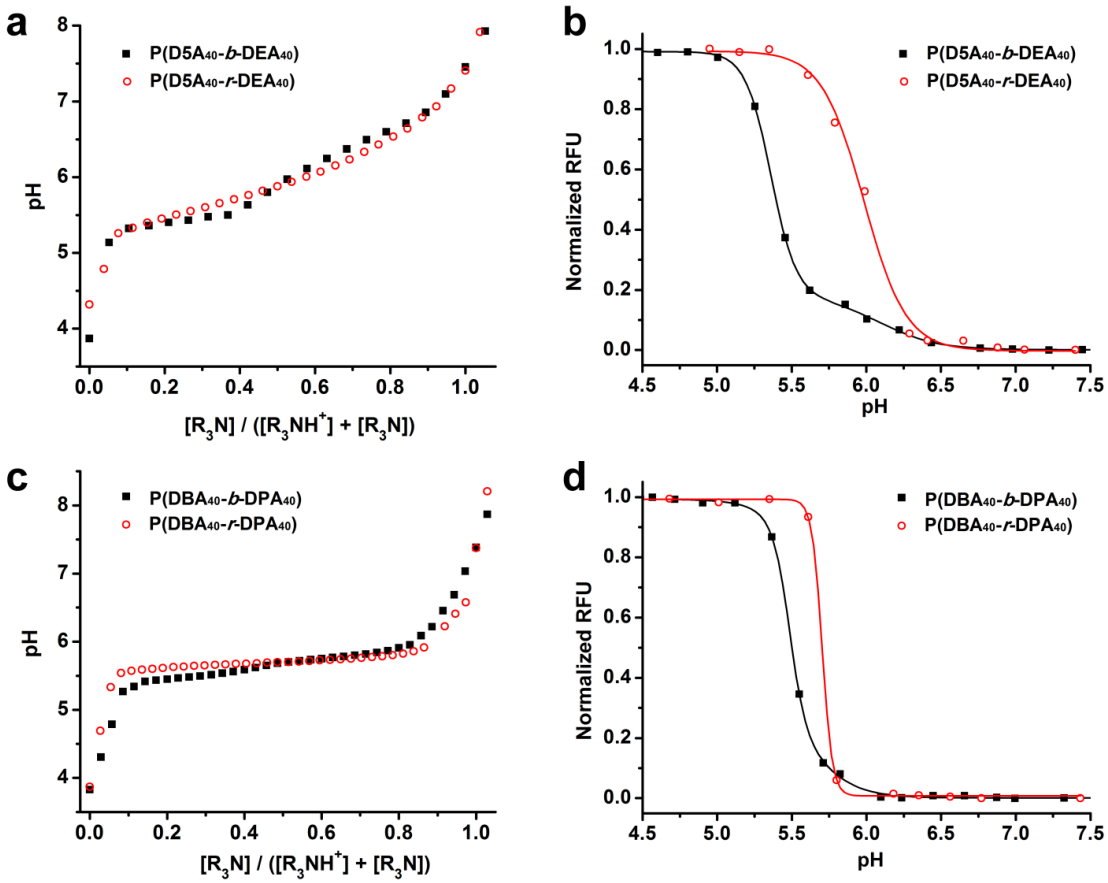

Figure S11. Comparison of the pH-responsive properties of two representative triblock copolymers with diblock copolymers with random PR segments. (**a**) pH titration curves for **P(D5A$_{40}$-*b*-DEA$_{40}$)** and **P(D5A$_{40}$-*r*-DEA$_{40}$)** copolymers as a function of molar fraction of tertiary amino groups. (**b**) Normalized fluorescence intensity as a function of pH for Cy5-conjugated **P(D5A$_{40}$-*b*-DEA$_{40}$)** and **P(D5A$_{40}$-*r*-DEA$_{40}$)** nanoprobes. (**c**) pH titration curves for **P(DBA$_{40}$-*b*-DPA$_{40}$)** and **P(DBA$_{40}$-*r*-DPA$_{40}$)** copolymers as a function of molar fraction of tertiary amino groups. (**d**) Normalized fluorescence intensity as a function of pH for Cy5-conjugated **P(DBA$_{40}$-*b*-DPA$_{40}$)** and **P(DBA$_{40}$-*r*-DPA$_{40}$)** nanoprobes.

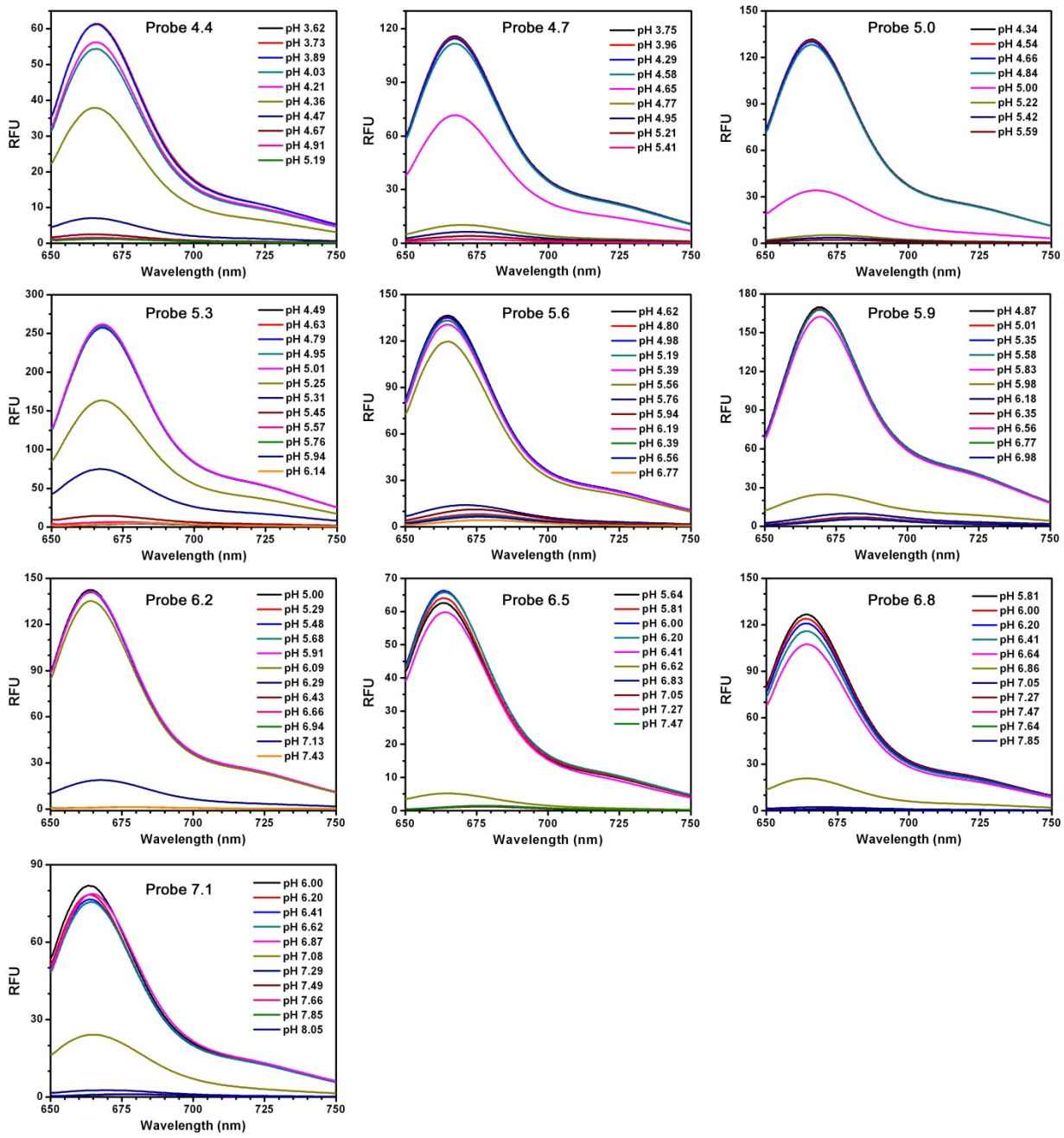

Figure S12. pH-dependent fluorescence spectra of the UPS library nanoprobes. The composition for each UPS nanoprobe was shown in Table S3. Cy5 dye ($\lambda_{ex}/\lambda_{em}$ = 646/662 nm) was conjugated to the PR blocks of the copolymers. The normalized fluorescence intensity vs. pH relationships were shown in **Figure 4d** in the main text.

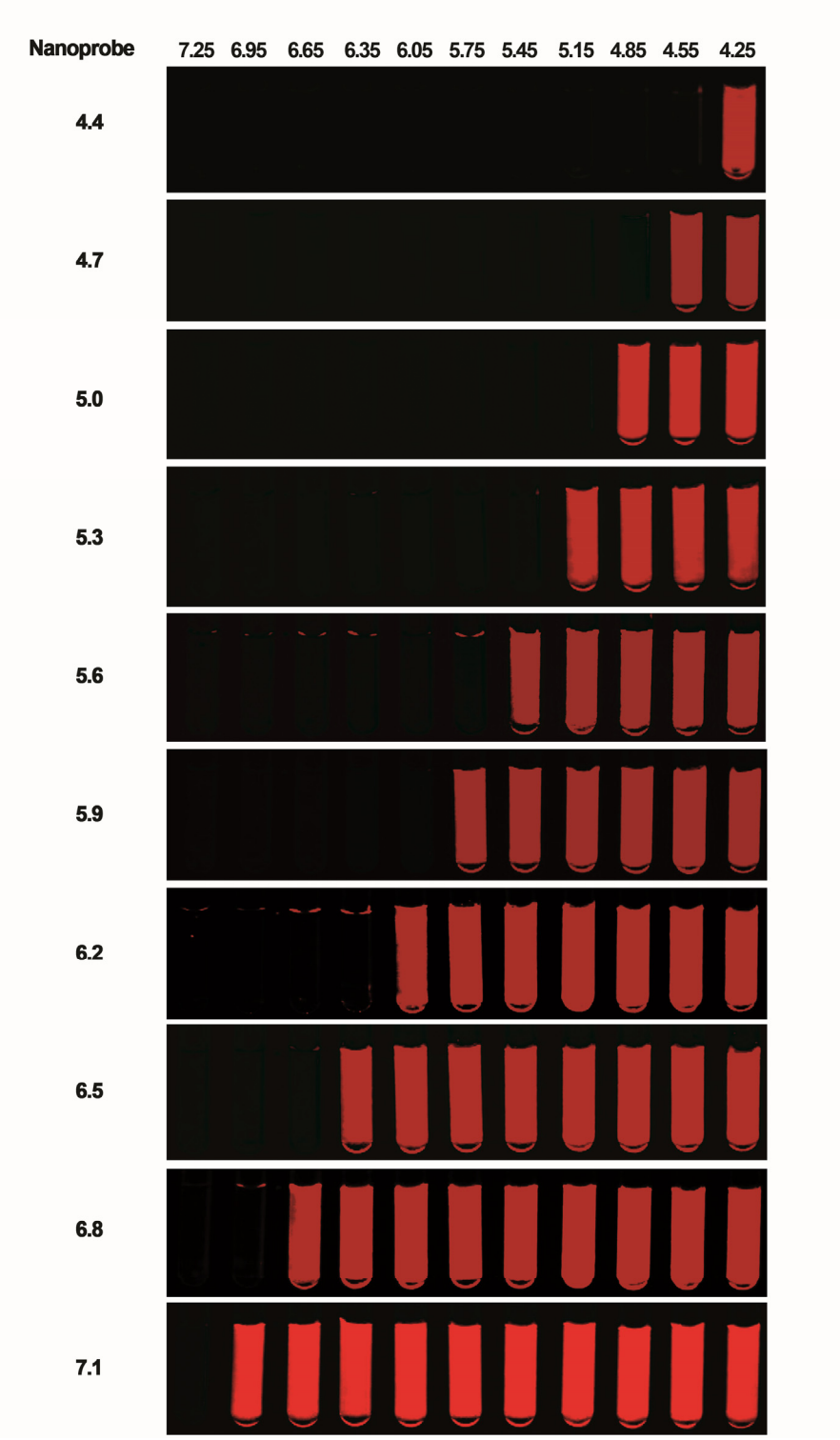

Figure S13. Fluorescence imaging of the UPS library consisting of 10 nanoprobes with 0.3 pH increment. The composition for each UPS nanoprobe was shown in Table S3. Cy5 dye ($\lambda_{ex}/\lambda_{em}$ = 646/662 nm) was conjugated to the PR blocks of the copolymers. Images of the nanoprobes were taken on a Maestro Imaging system.

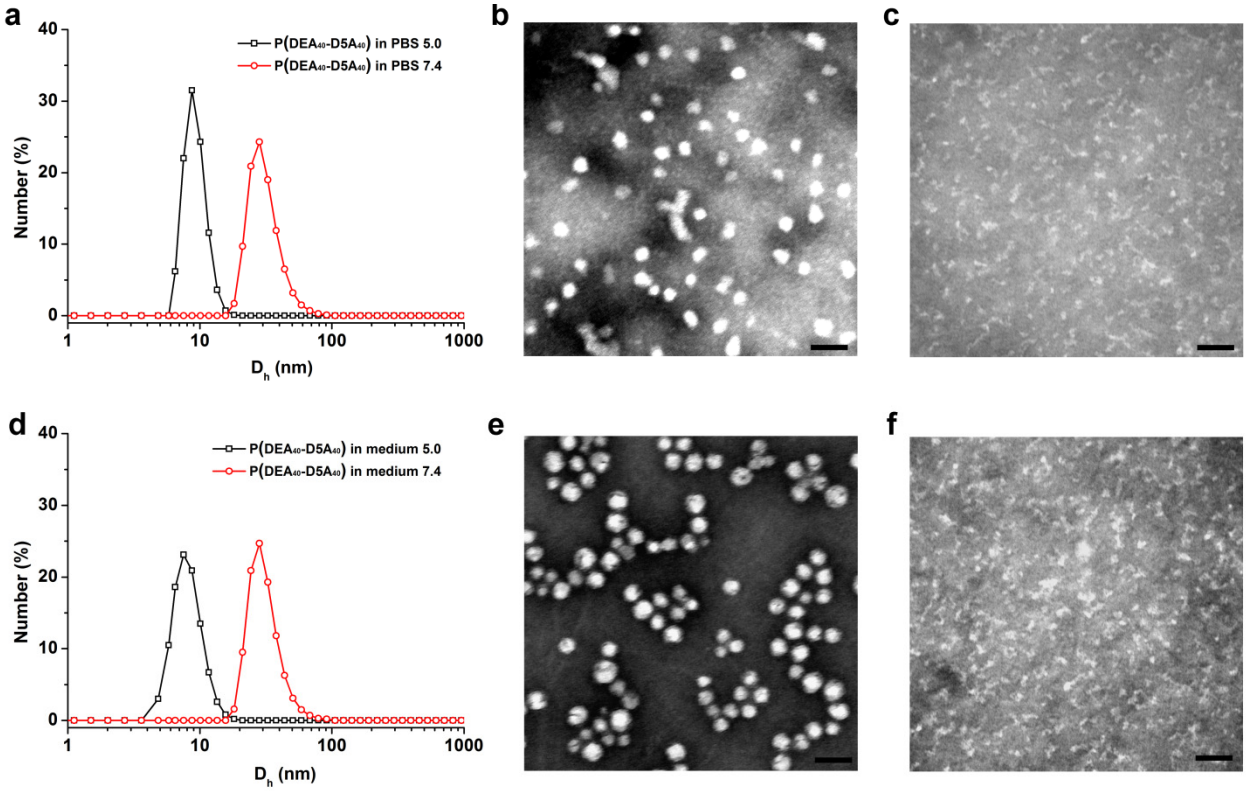

Figure S14. Characterization of **P(DEA$_{40}$-D5A$_{40}$)** nanoprobes. (**a**) DLS histograms of **P(DEA$_{40}$-D5A$_{40}$)** nanoprobes as micelles in pH 7.4 PBS solution and as unimers in pH 5.0 PBS solution. (**b, c**) TEM image of **P(DEA$_{40}$-D5A$_{40}$)** nanoprobes from pH 7.4 and 5.0 solutions, respectively. Scale bars = 50 nm. (**d**) DLS histograms of **P(DEA$_{40}$-D5A$_{40}$)** nanoprobes as micelles in pH 7.4 and as unimers in pH 5.0 solution of cell culture medium containing 10% FBS. (**e, f**) TEM image of **P(DEA$_{40}$-D5A$_{40}$)** nanoprobes in pH 7.4 and pH 5.0 solutions of cell culture medium containing 10% FBS, respectively. Scale bars = 50 nm.

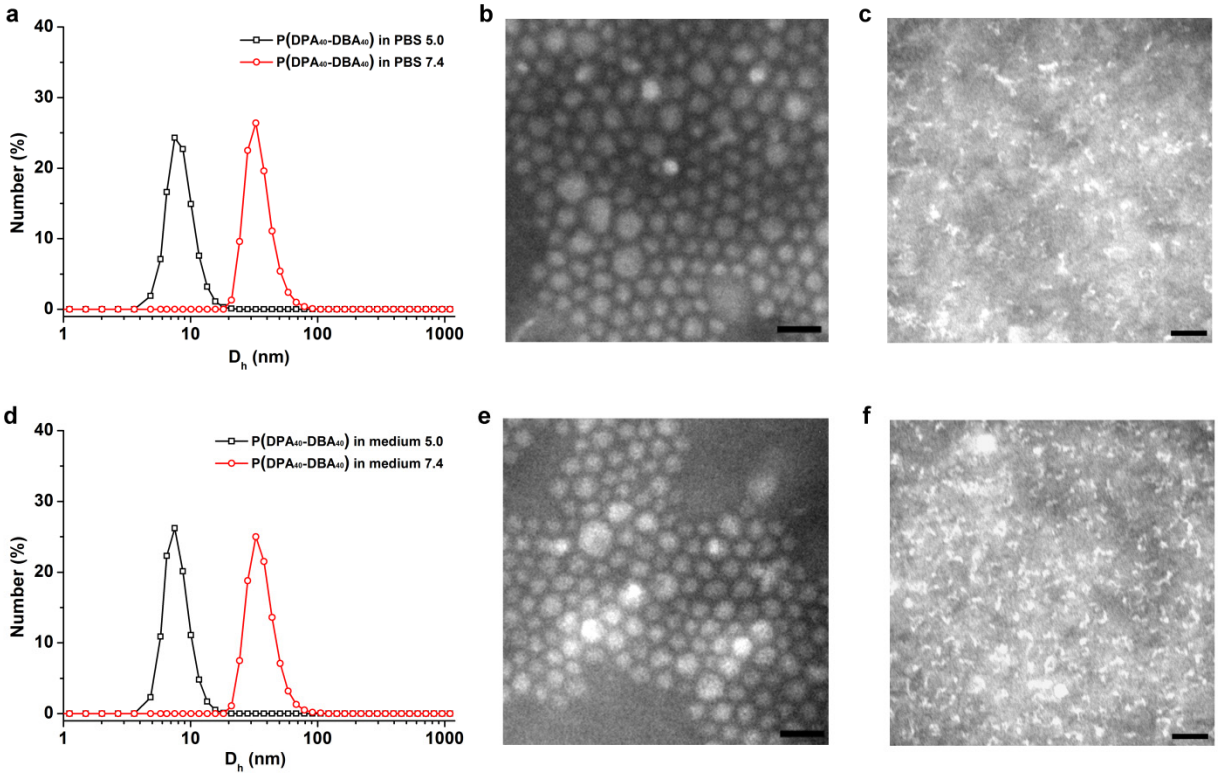

Figure S15. Characterization of **P(DPA$_{40}$-DBA$_{40}$)** nanoprobes. (**a**) DLS histograms of **P(DPA$_{40}$-DBA$_{40}$)** nanoprobes as micelles in pH 7.4 PBS solution and as unimers in pH 5.0 PBS solution. (**b, c**) TEM image of **P(DPA$_{40}$-DBA$_{40}$)** nanoprobes from pH 7.4 and 5.0 solutions, respectively. Scale bars = 50 nm. (**d**) DLS histograms of **P(DPA$_{40}$-DBA$_{40}$)** nanoprobes as micelles in pH 7.4 and as unimers in pH 5.0 solution of cell culture medium containing 10% FBS. (**e, f**) TEM image of **P(DPA$_{40}$-DBA$_{40}$)** nanoprobes in pH 7.4 and pH 5.0 solutions of cell culture medium containing 10% FBS, respectively. Scale bars = 50 nm.

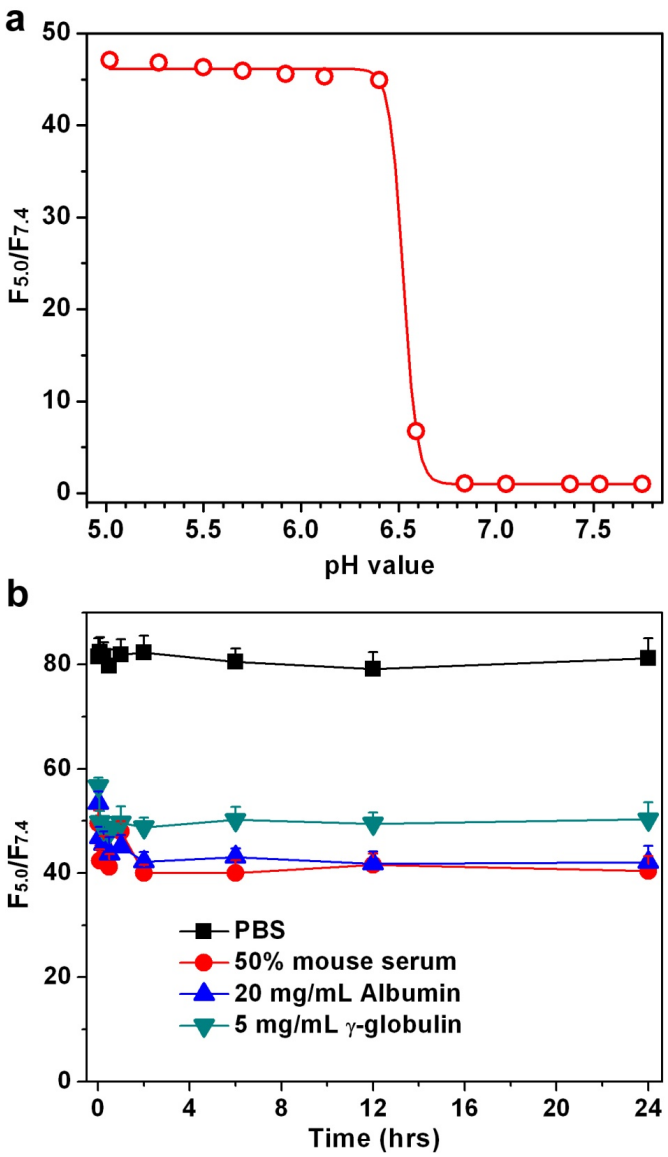

Figure S16. Evaluation of stability of nanoprobes under serum conditions. (**a**) Fluorescence ratio as a function of pH for **6.5-TMR** (**P(DEA$_{21}$-DPA$_{79}$)**) nanoprobe in the presence of 10% fetal bovine serum (FBS) in the cell culture medium. (**b**) Fluorescence on/off ratios of **6.5-TMR** nanoprobe in fresh mouse serum or solutions containing mouse serum components.

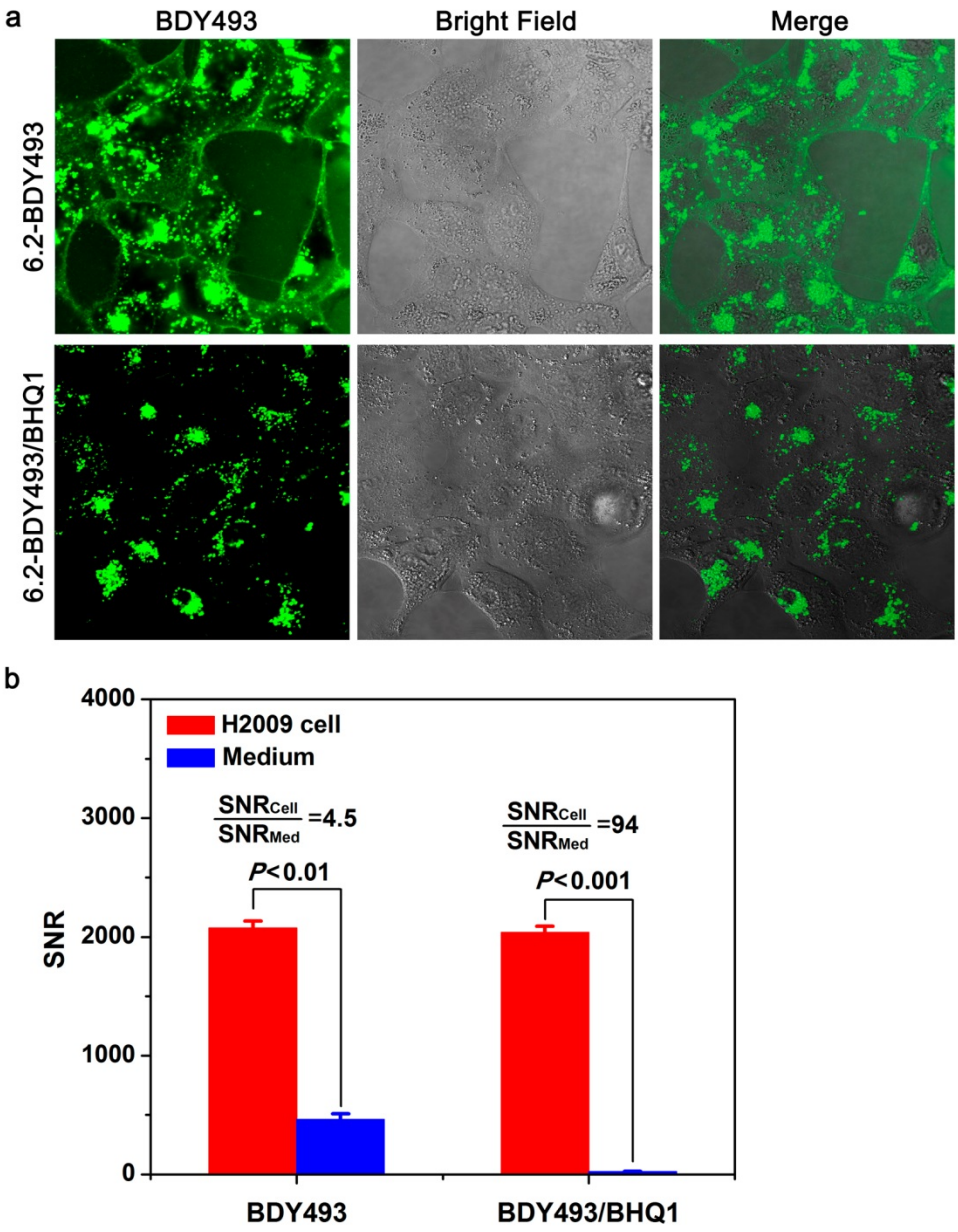

Figure S17. *In vitro* confocal imaging of H2009 lung cancer cells with **6.2-BDY493** and (**6.2-BDY493/BHQ1**) nanoprobes. (**a**) Representative confocal images of nanoprobes in H2009 cells. For the (**6.2-BDY493/BHQ1**) nanoprobes, the medium background signal is low and most nanoprobe signals come from activated nanoprobes in the acidic endosomes/lysosomes. (**b**) Quantitative analysis of signal to noise ratios (SNRs) of nanoprobes inside H2009 cells and medium background for the **6.2-BDY493** and (**6.2-BDY493/BHQ1**) nanoprobes. *P*-values are calculated using the Student's t-test.

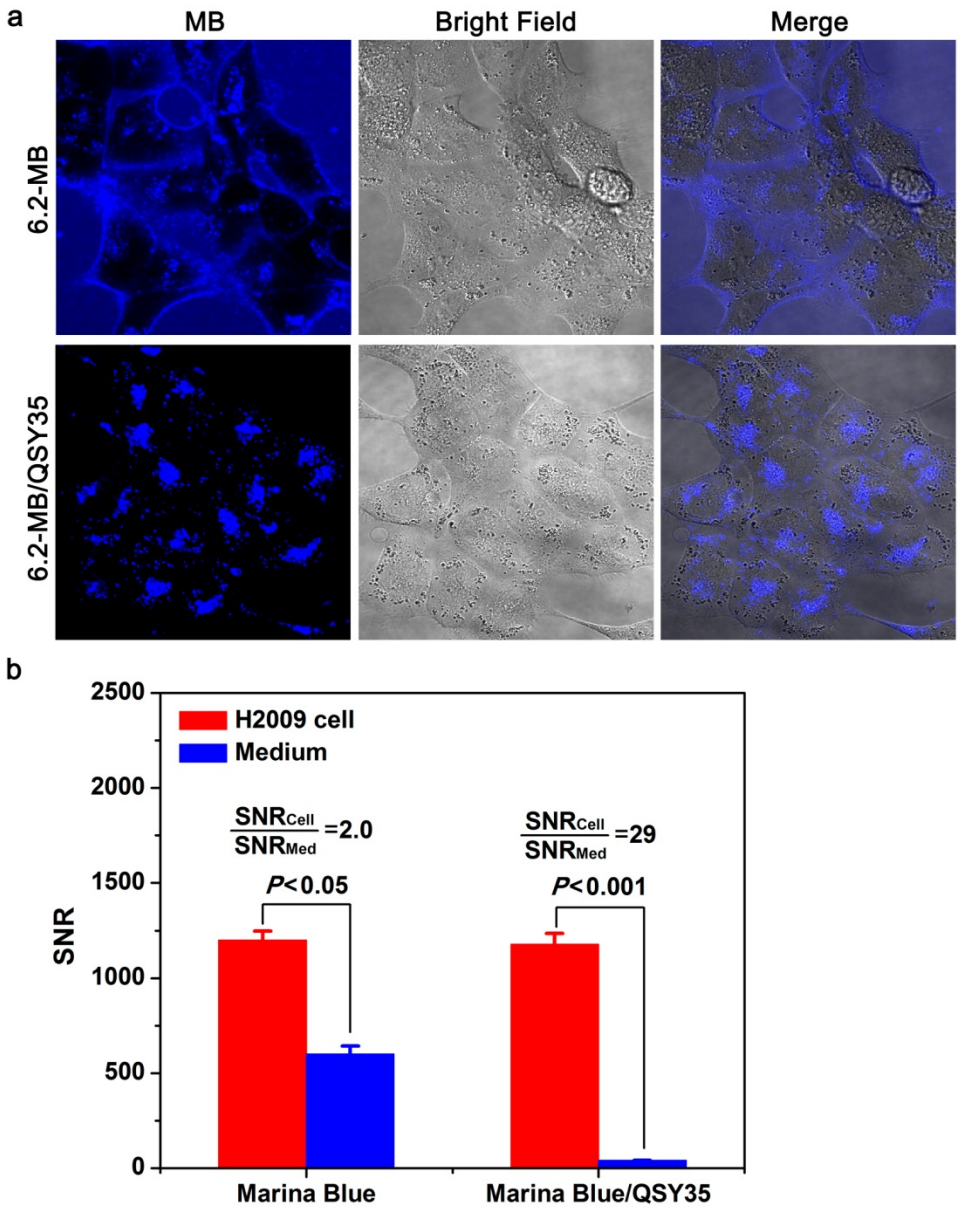

Figure S18. *In vitro* confocal imaging of H2009 lung cancer cells with **6.2-MB** and (**6.2-MB/QSY35**) nanoprobes. (**a**) Representative confocal images of nanoprobes in H2009 cells. For the (**6.2-MB/QSY35**) nanoprobes, the medium background signal is low and most nanoprobe signals come from activated nanoprobes in the acidic endosomes/lysosomes. (**b**) Quantitative analysis of signal to noise ratios (SNRs) of nanoprobes inside H2009 cells and medium background for the **6.2-MB** and (**6.2-MB/QSY35**) nanoprobes. *P*-values are calculated using the Student's t-test.

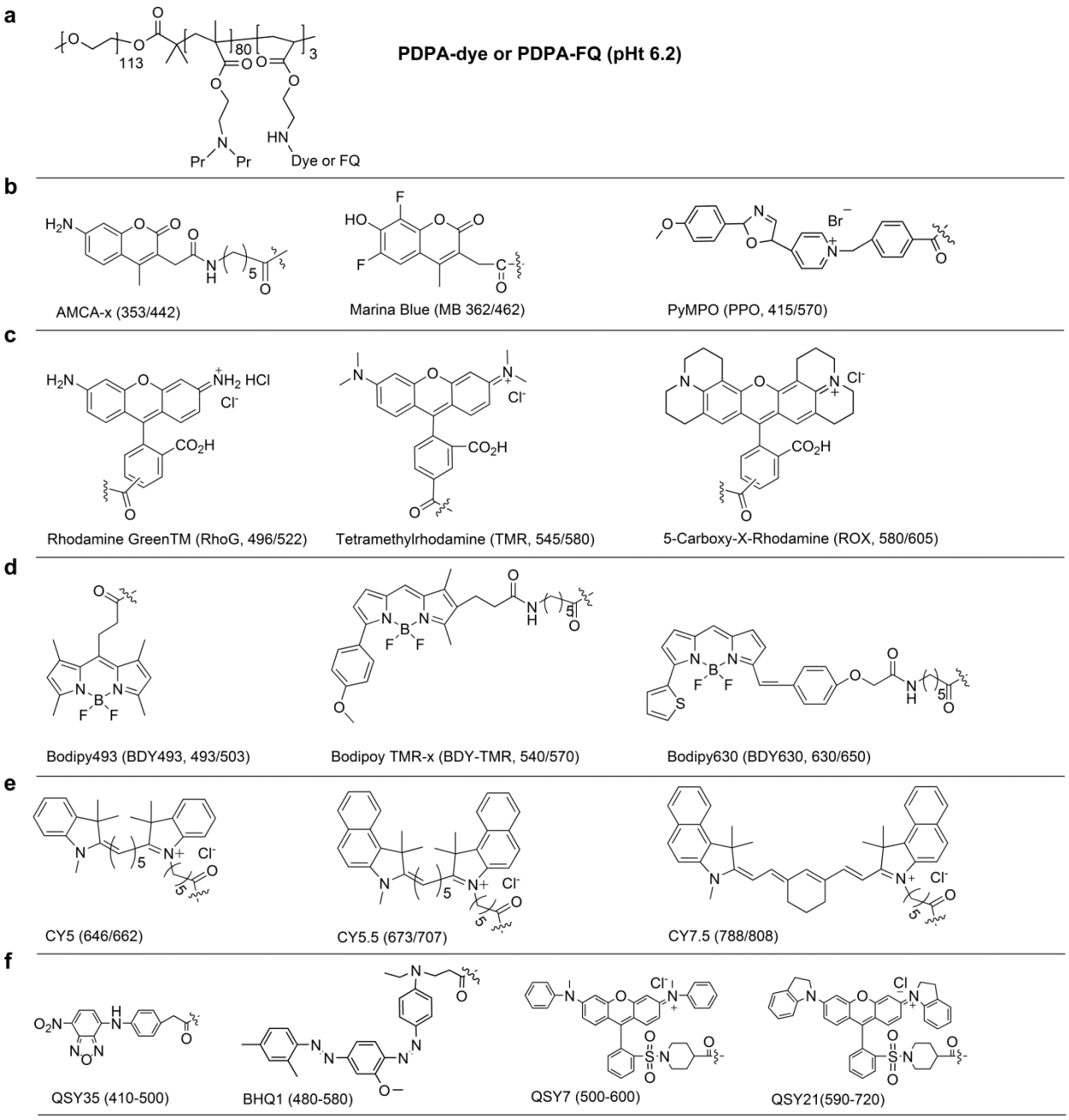

Figure S19. (**a**) Structures of the PEO-PDPA-Dye/FQ copolymers. (**b**)Structures of selected fluorophores with large Stokes shift. (**c**) Structures of selected Rhodamine dyes. (**d**) Structures of selected BODIPY dyes. (**e**) Structures of selected cyanine dyes. The excitation/emission wavelengths for all the fluorophores were shown in parenthesis in **b-e**, respectively. (**f**) Structures of the selected fluorescence quenchers. The active quenching range of each quencher was shown in parenthesis.

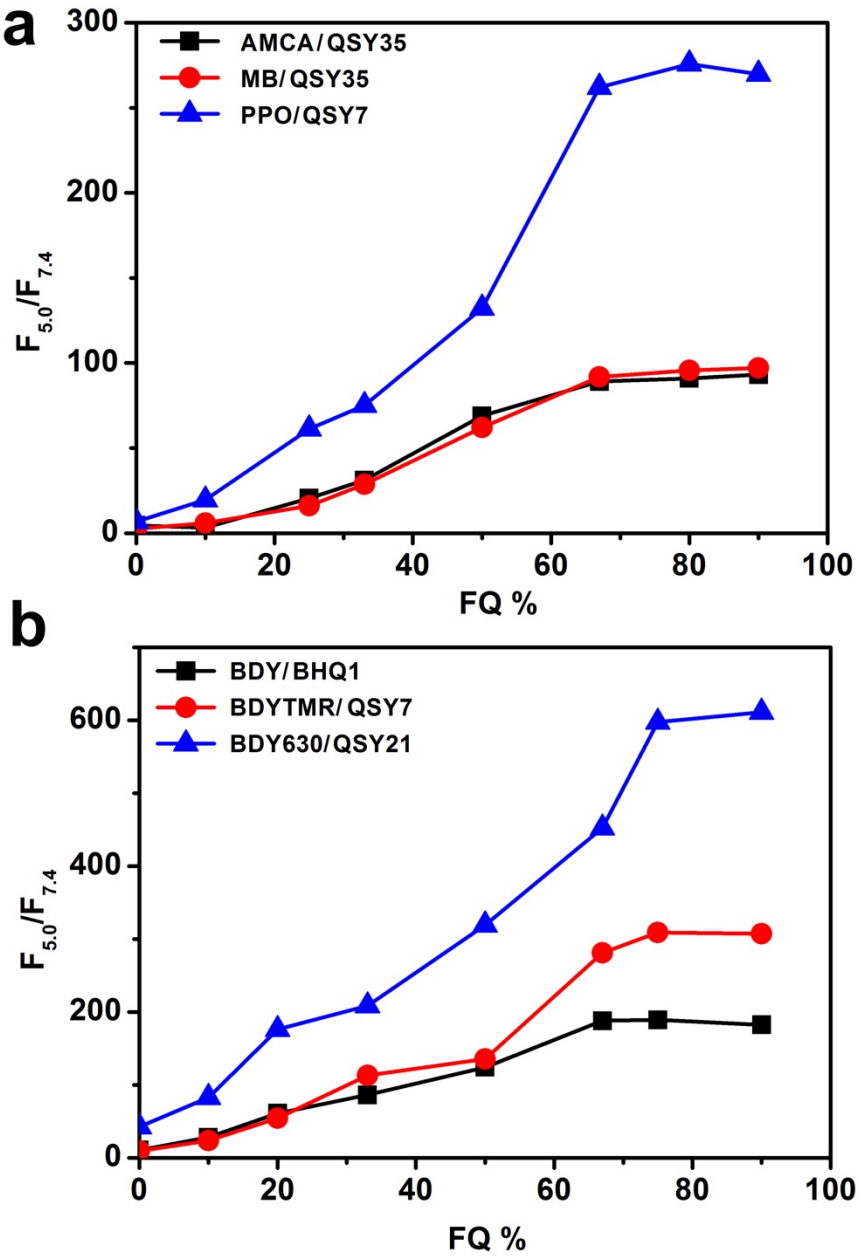

Figure S20. Fluorescence intensity ratios of mixed nanoparticles at pH 5.0 (ON) and pH 7.4 (OFF) at different ratios of (**PDPA-Dye**/**PDPA-FQ**). (**a**) Results for fluorophores with large Stokes shift (AMCA, MB and PPO). (**b**) Results for BODIPY families of fluorophores. The structures of the fluorophores and FQs were shown in **Figure S19**.

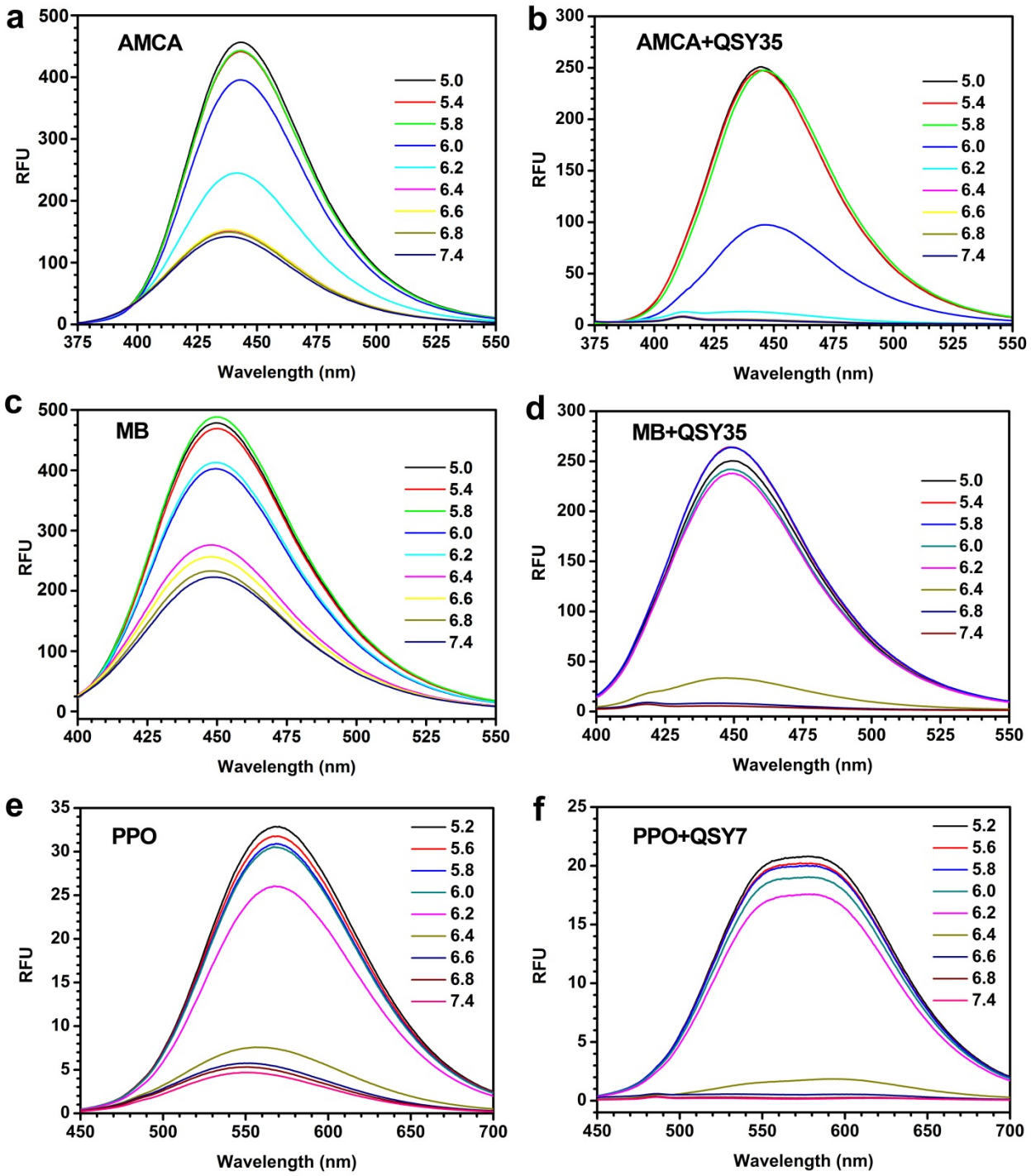

Figure S21. pH-dependent fluorescence spectra of nanoprobes without (left column) or with (right column) fluorescence quenchers. Fluorophores with large Stokes shift were presented in this study. The structures of the fluorophores and FQs were shown in **Figure S19**.

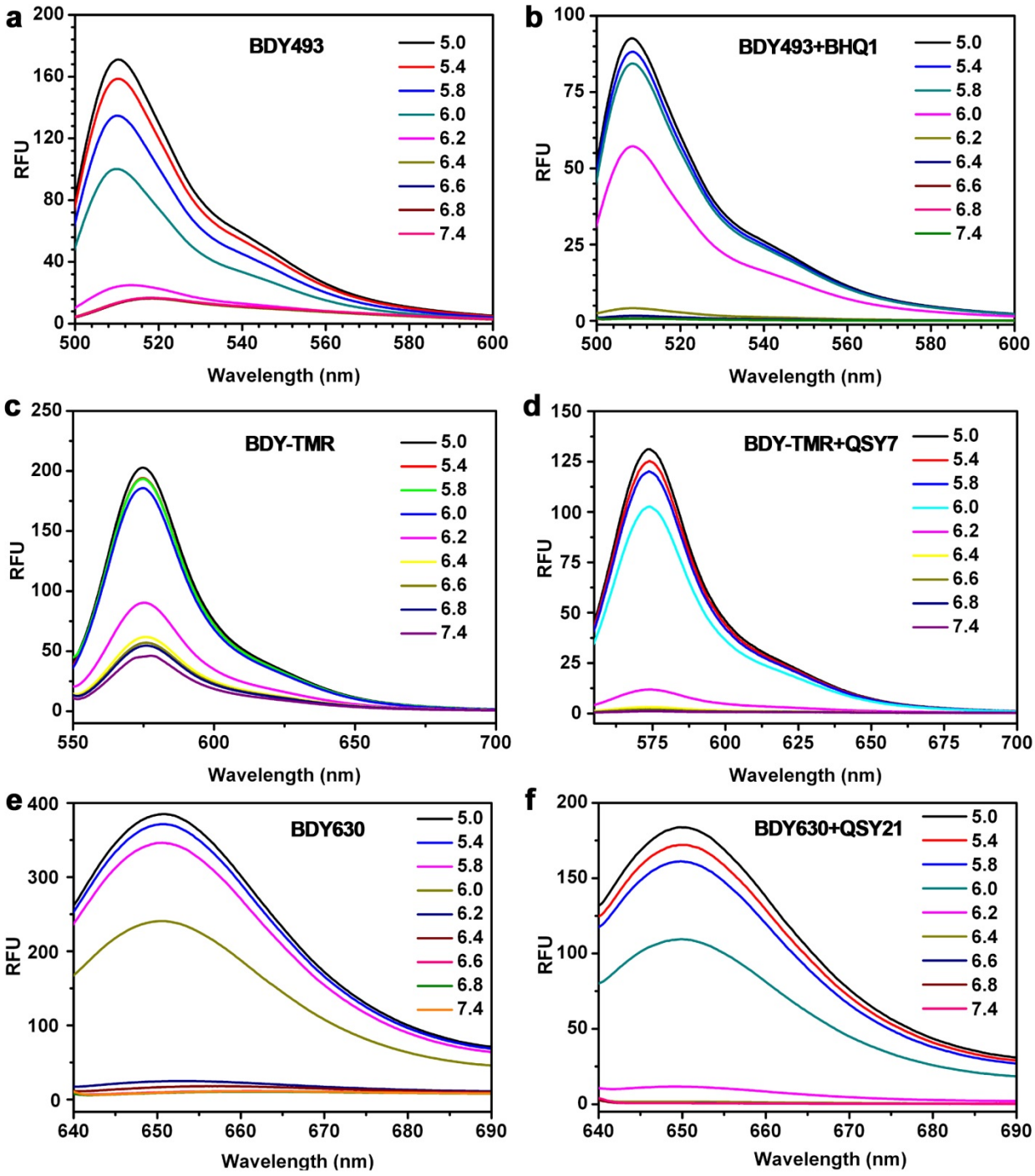

Figure S22. pH-dependent fluorescence spectra of nanoprobes without (left column) or with (right column) fluorescence quenchers. BODIPY family of fluorophores was presented in this study. The structures of the fluorophores and FQs were shown in **Figure S19**.

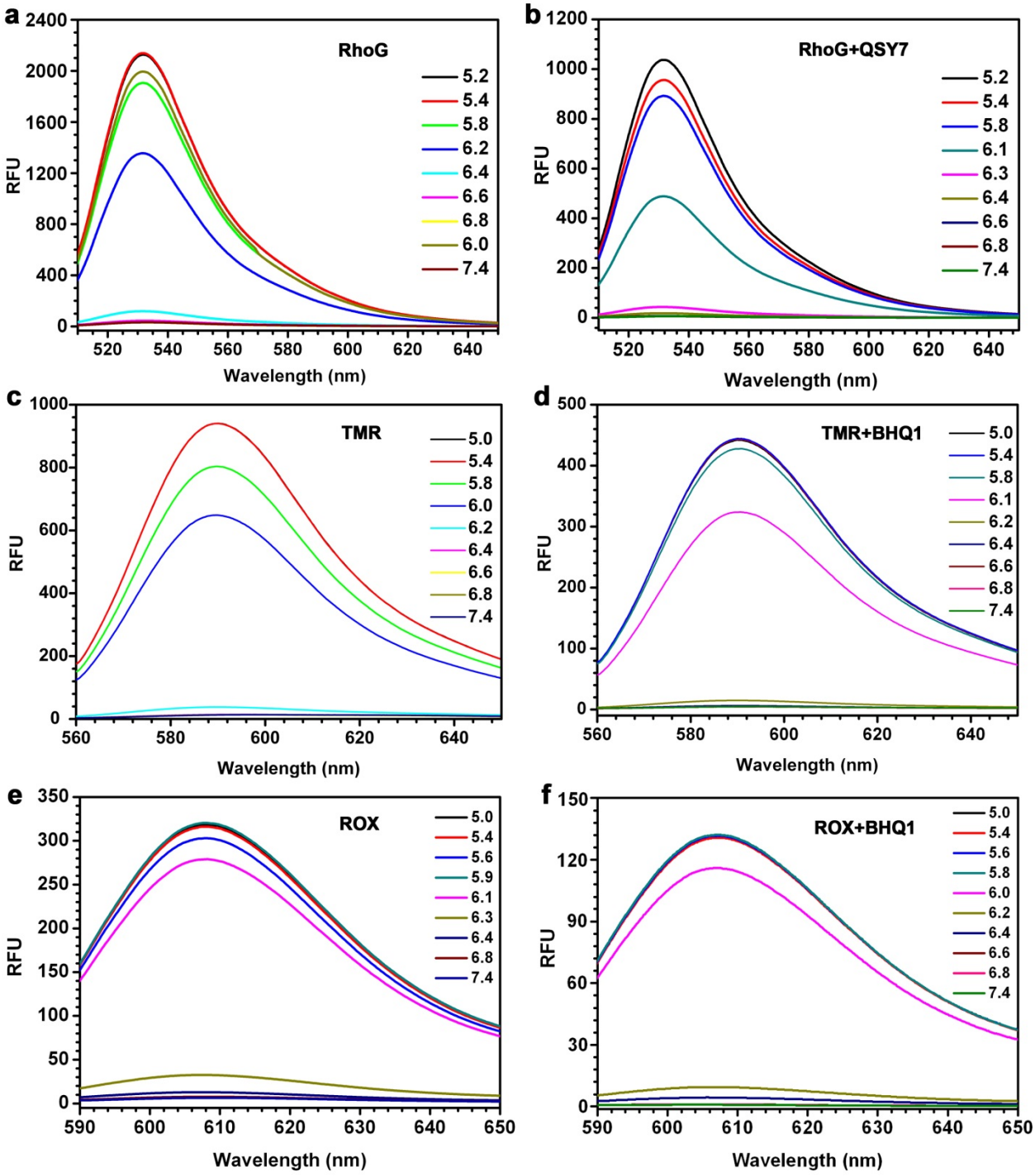

Figure S23. pH-dependent fluorescence spectra of nanoprobes without (left column) or with (right column) fluorescence quenchers. Rhodamine family of fluorophores was presented in this study. The structures of the fluorophores and FQs were shown in **Figure S19**.

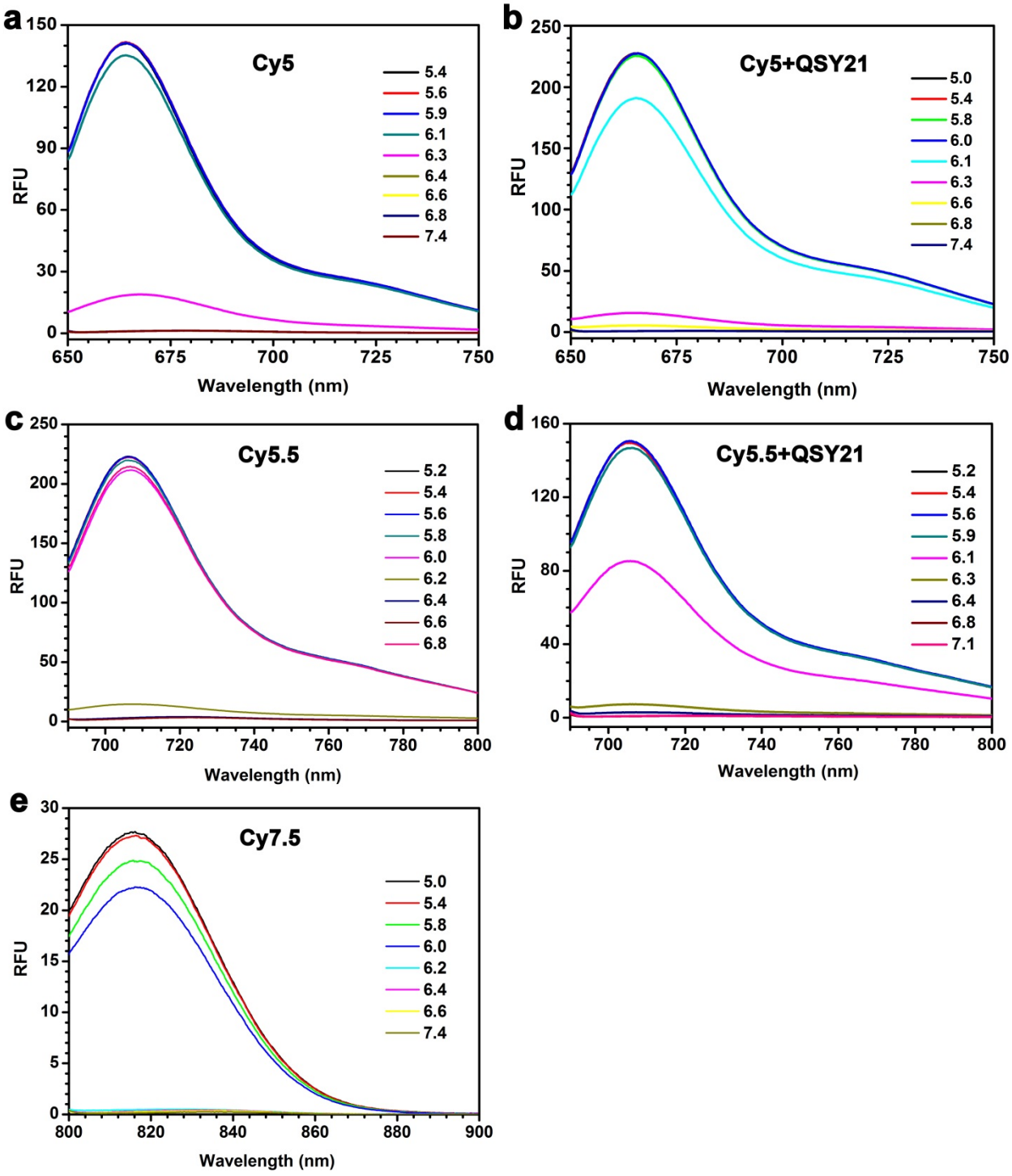

Figure S24. pH-dependent fluorescence spectra of nanoprobes without (left column) or with (right column) fluorescence quenchers. Cyanine family of fluorophores was presented in this study. The structures of the fluorophores and FQs were shown in **Figure S19**.

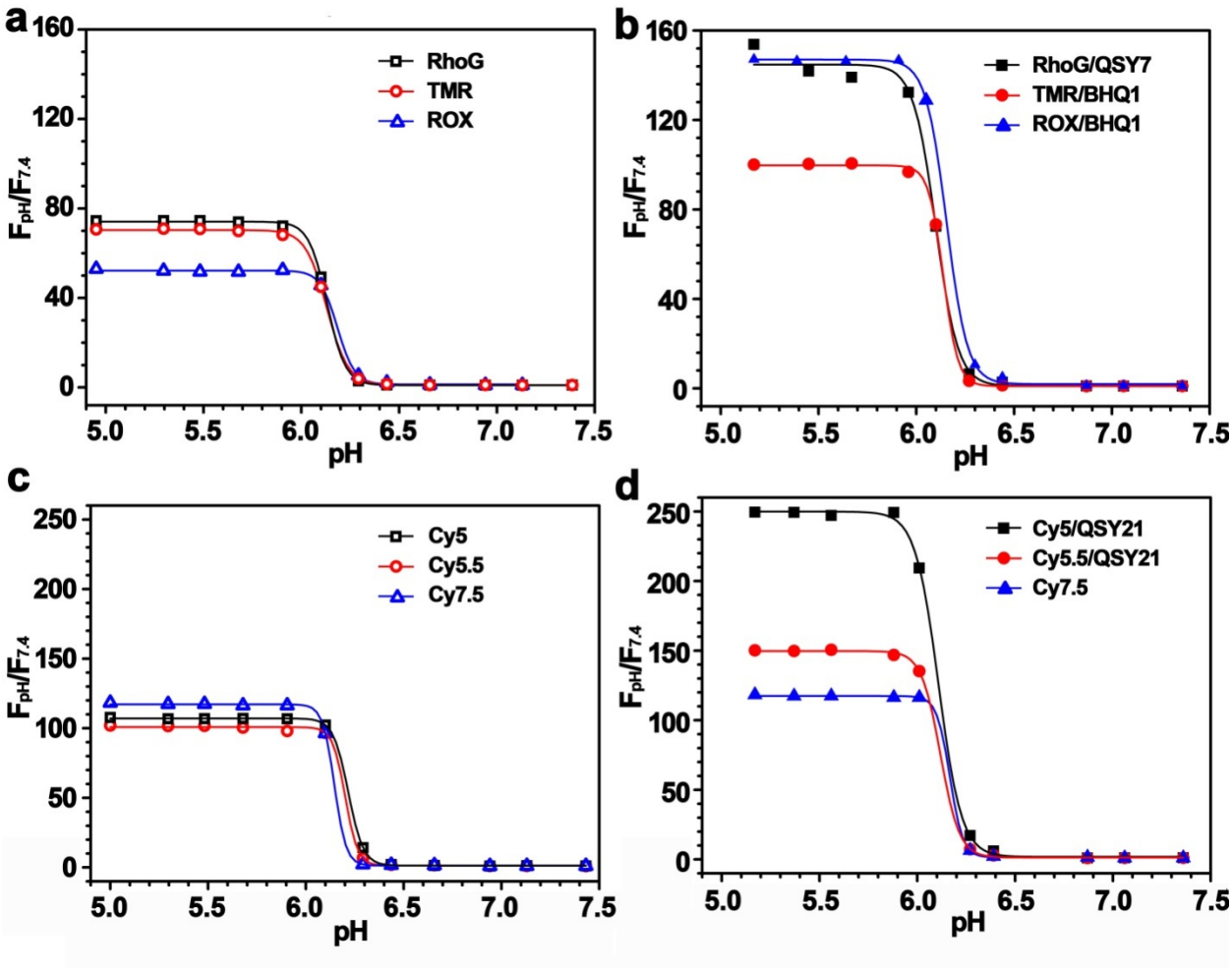

Figure S25. Fluorescence intensity ratio at different pH to pH 7.4 ($F_{pH}/F_{7.4}$) was plotted for copolymer alone (**a, c**) and with the addition of FQ-conjugated copolymers (**b, d**) for Rhodamine and Cyanine families of dyes. See main text for detailed description and **Fig. S19** for the structures of the dyes and FQs.

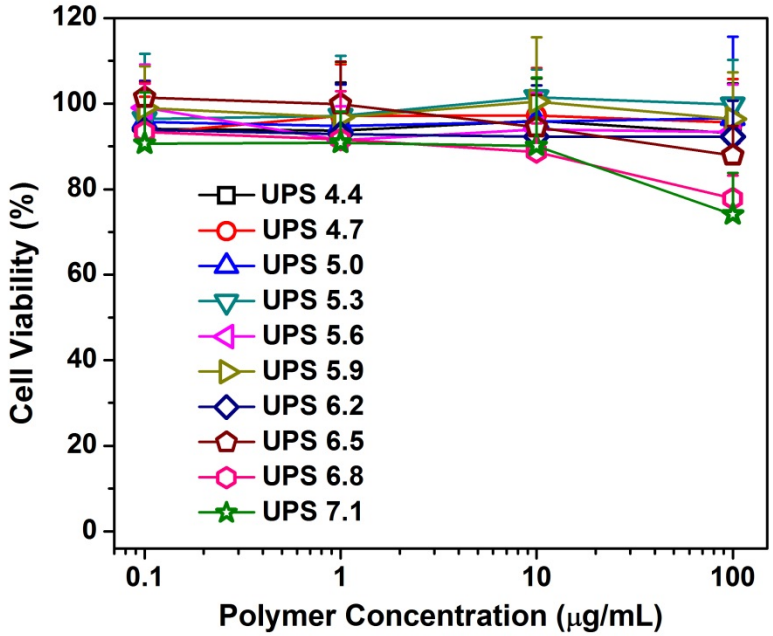

Figure S26. Evaluation of the cytotoxicity of UPS nanoprobes in H2009 lung cancer cells. H2009 cells were exposed to ten UPS nanoprobes with different pH_t for 4 hours at 37 ºC. The cell viability was evaluated by the MTT assay after 48 hours incubation. Error bars represent standard deviation of four replicate samples.